การจำลองการปลูกผลึกแบบโมเลกุลาร์บีมเอพิแทกซีภายใต้ผลของกำแพงศักย์แบบ Ehrlich-Schwoebel

นายสุนทร จรรยาวดี

วิทยานิพนธ์นี้เป็นส่วนหนึ่งของการศึกษาตามหลักสูตรปริญญาวิทยาศาสตรมหาบัณฑิต
สาขาวิชาฟิสิกส์ ภาควิชาฟิสิกส์
คณะวิทยาศาสตร์ จุฬาลงกรณ์มหาวิทยาลัย
ปีการศึกษา 2547

ISBN 974-17-6662-9

MODELING OF MOLECULAR BEAM EPITAXY GROWTH UNDER EHRLICH-SCHWOEBEL POTENTIAL BARRIER EFFECTS

Mr. Soontorn Chanyawadee

A Thesis Submitted in Partial Fulfillment of the Requirements
for the Degree of Master of Science in Physics

Department of Physics
Faculty of Science
Chulalongkorn University

Academic year 2004
ISBN 974-17-6662-9

Thesis Title	Modeling of molecular beam epitaxy growth under Ehrlich-Schwoebel potential barrier effects
By	Mr. Soontorn Chanyawadee
Field of Study	Physics
Thesis Advisor	Patcha Chatraphorn, Ph.D.

Accepted by the Faculty of Science, Chulalongkorn University in Partial Fulfillment of the Requirements for the Master's Degree

..... Dean of the Faculty of Science
(Professor Piamsak Menasveta, Ph.D.)

THESIS COMMITTEE

..... Chairman
(Assistant Professor Kiranant Ratanathammapan)

..... Thesis Advisor
(Patcha Chatraphorn, Ph.D.)

..... Member
(Varagorn Piputnchonlathee, Ph.D.)

..... Member
(Sakuntam Sanorpim, Ph.D.)

สุนทร จรรยาวดี : การจำลองการปลูกผลึกแบบโมเลกุลาร์บีมเอพิแทกซีภายใต้ผลของกำแพงศักย์แบบ Ehrlich-Schwoebel. (MODELING OF MOLECULAR BEAM EPITAXY GROWTH UNDER EHRLICH-SCHWOEBEL POTENTIAL BARRIER EFFECTS) อ. ที่ปรึกษา : ดร. ปัจฉา ฉัตราภรณ์, 53 หน้า. ISBN 974-17-6662-9.

ในการปลูกฟิล์มแบบโมเลกุลาร์บีมเอพิแทกซี (เอ็มบีอี) อะตอมมีโอกาสที่จะเจอตำแหน่งที่ฟิล์มมีความสูงต่างกันขณะเคลื่อนที่อยู่บนผิวของฟิล์ม โดยอะตอมจะต้องผ่านกำแพงศักย์ขณะที่เคลื่อนที่จากชั้นที่ฟิล์มมีความสูงมากกว่าลงมายังชั้นที่มีความสูงน้อยกว่า กำแพงศักย์นี้เรียกว่ากำแพงศักย์ Ehrlich-Schwoebel (ES) ในงานนี้ได้ศึกษาถึงผลของกำแพงศักย์แบบ ES ที่มีต่อการปลูกฟิล์มแบบเอ็มบีอี โดยใช้แบบจำลองเอ็มบีอีซึ่งเป็นแบบจำลองแบบไม่ต่อเนื่อง บนแผ่นรองรับหนึ่งมิติ จากการศึกษาพบว่าเกิดเนิน (mound) ขึ้นที่ผิวของฟิล์มโดยเป็นกลุ่มขนาดใหญ่เมื่อกำแพงศักย์มีค่าน้อย และจะมีขนาดเล็กเมื่อกำแพงศักย์มีค่ามาก การศึกษาสมบัติของกลุ่มอะตอม เช่น รัศมีเฉลี่ยและความสูงเฉลี่ย ที่เปลี่ยนแปลงตามเวลาทำให้สามารถแบ่งกระบวนการปลูกฟิล์มได้เป็นสองช่วง ในช่วงแรกกลุ่มของอะตอมแต่ละกลุ่มจะรวมตัวกันทำให้รัศมีของกลุ่มอะตอมมีค่าเพิ่มขึ้น ต่อจากนั้นในช่วงที่สอง การรวมตัวกันของกลุ่มอะตอมจะช้ามากทำให้รัศมีของกลุ่มอะตอมมีค่าเกือบจะคงที่ และอะตอมที่มาจากจากแหล่งกำเนิดจะรวมตัวเป็นฟิล์มที่ส่วนบนของกลุ่มอะตอมเหล่านั้น ทำให้ความสูงเฉลี่ยของกลุ่มอะตอมเพิ่มขึ้นตลอดกระบวนการปลูกฟิล์ม

ภาควิชา ฟิสิกส์ ลายมือชื่อนิสิต.....
สาขาวิชา ฟิสิกส์ ลายมือชื่ออาจารย์ที่ปรึกษา.....
ปีการศึกษา 2547

4572542223 :MAJOR PHYSICS
KEY WORDS: ES BARRIER / MBE MODEL / MOUND

SOONTORN CHANYAWADEE : MODELING OF MOLECULAR BEAM EPITAXY GROWTH UNDER EHRLICH-SCHWOEBEL POTENTIAL BARRIER EFFECTS. THESIS ADVISOR : PATCHA CHATRAPHORN, PH.D., 53 pp. ISBN 974-17-6662-9.

In molecular beam epitaxy (MBE) film growing, atoms may encounter a step edge – a region where two terraces of different height meet – while diffusing across the growth front. A diffusing atom must overcome an additional potential barrier when hopping down from the upper terrace to the lower one. This barrier is known as the Ehrlich-Schwoebel (ES) barrier. In this work, a discrete MBE model on one-dimensional substrate is used to determine effects of the ES barrier on MBE growth. We found mound formation on the grown surface with larger mound structure in weaker barrier systems and smaller mounds in stronger ones. The study of the time evolution of mound properties such as the average mound radius and the average mound height shows that this growth process can be divided into two stages. In the initial stage, individual mound coarsens resulting in the increase of the mound radius. In the second stage at later time, coarsening process becomes very slow and the mound radius is approximately constant. With mound radius fixed as a constant in time, newly deposited atoms are incorporated on top of existing mounds and the average mound height increases as growth time increases.

Department Physics — Student's signature .....

Field of study Physics — Advisor's signature .....

Academic year 2004

Acknowledgements

I would like to express my deepest gratitude and appreciation to my advisor, Dr. Patcha Chatraphorn, for her kindness suggestion. I am also grateful to Assistant Professor Kiranant Ratanathammapan, Dr. Varagorn Piputnchonlathee and Dr. Sakuntam Sanorpim for serving as a chairman and the committee respectively. All of whom have made valuable comments and have been helpful in the production of this thesis.

The research described in this thesis was supported financially by the Development and Promotion of Science and Technology Talents Project (DPST), and it is my great pleasure to thank some of the people who have helped me in various ways.

Many thanks go to my friends and colleagues, whose names are not mentioned here, who have contributed suggestions and courteous assistance during the work.

Finally, a deep affectionate gratitude is acknowledged to my family for love, understanding, and encouragement throughout the entire study.

Table of Contents

List of Tables

List of Figures

Chapter 1

Introduction

Crystal growth, particularly high-quality epitaxial thin film growth, is one of very interesting topics impacting today's technology. A major issue in crystal growth is to have a dynamical control over the growth process to obtain a thin film with certain desired patterns. Thus, in order to be able to design a controlled growth process, it is important to understand the nature of instabilities [1, 2, 3, 4, 5] that destroy controllability during a growth process. Ehrlich-Schwoebel (ES) barrier [6, 7], one of those instabilities, is a ubiquitous phenomenon in real experimental surface growth. An ES barrier produces an additional energy barrier which inhibits diffusing atoms on upper terraces from coming down toward lower levels. Therefore, this barrier enhances diffusing atoms to move toward upper terraces and the result is mound formation. In this research, we used a discrete growth model called MBE model [8, 9, 10] to simulate molecular beam epitaxy (MBE) growth under effects of an ES barrier. Mound properties such as an average mound radius and an average mound height were investigated via the study of height-height correlation function [11, 12].

In the next chapter, Chapter 2, we will describe theoretical background needed for our computational MBE growth studies. In addition, several useful models used in computer simulations such as the random deposition (RD) model, the Das Sarma-Tamborenea (DT) model, and the MBE model will be explained. Since the MBE model is more realistic, it is the model selected in this thesis.

We will present our numerical results of the MBE growth in Chapter 3.

In this chapter, morphologies at various substrate temperatures and the scaling properties of the model will be shown. Moreover, the relation between the surface diffusion length and the substrate temperature will be shown in the last section.

In Chapter 4, we modified the basic MBE model to include effects of the ES barrier. The barrier causes mound formation in the evolving surfaces. The time evolution of mound properties such as an average mound radius and an average mound height was observed by studying the height-height correlation function. Finally, the last chapter, Chapter 5, is the conclusions of this thesis.

Chapter 2

Theoretical Aspects and Models

In this chapter, we will talk about the theoretical background needed for our work. First, the molecular beam epitaxy growth is described by showing its fundamental processes, i.e. deposition, desorption, and surface diffusion process. Second, models that have been proposed to describe kinetic roughening phenomena in surface growth such as the RD model, the DT model, and the MBE model are presented. Finally, we introduce the dynamical scaling hypothesis which we use to study the kinetic roughening phenomena of the surface growth.

2.1 Molecular Beam Epitaxy Growth

Among numerous crystal growth techniques, MBE is a good choice to obtain high quality films for variety of materials including both metal and semiconductor. In addition, films grown by MBE rarely contain any bulk vacancy [9, 13, 14]. In this technique, a flat singular substrate is held at a constant temperature in a vacuum chamber with ultra-high pressure, i.e. smaller than 10^{-10} torr, to minimize the impurities such as H_2, CO_2, CO and H_2O within the growth environment [13]. The temperature of the substrate is usually in the range between 500 K to 1000 K. Beams of materials to be grown are generated by thermal evaporation from various sources and directed perpendicularly to the substrate. Thickness of the film is controlled by deposition rate, number of layers grown in a unit time, and time used in the growth process.

From microscopic point of view, the fundamental phenomena of the MBE growth are the interplay between deposition, desorption and surface diffusion process [13].

2.1.1 Deposition

During the deposition process, an atom from the beam is deposited on a random position of the substrate, forms bonds with surface atoms, and then sticks there. If the substrate and the film are of the same material, it is called a homoepitaxy growth. Otherwise, in the case when the substrate and the film are different, the growth process is a heteroepitaxy growth. In heteroepitaxy growth, strain due to the difference in lattice constant of substrate and film materials has a crucial effect on the growth process. In this thesis, however, we are only interested in homoepitaxy growth. The deposition rate, which plays an important role in determining properties of the grown film, is calculated from the number of monolayers (ML) grown in a unit time (ML/s).

2.1.2 Desorption

Desorption is the process that some surface atoms leave the growing surface by breaking bonds formed with other atoms. The desorption probability depends on the number and the strength of bonds that the atom possesses. For example, an atom with strong bonds have less chance to leave the surface compared with an atom with weaker bonds. Similarly, it is more difficult for an atom with many bonds, e.g. atoms at kinks or pits, to desorp when compared with atoms with fewer bonding. (Note that conventionally, a kink/pit means a site where an atom can form one/two lateral bonds.) However, desorption rate is usually extremely small under typical MBE conditions that it can be considered negligible. So in this work, desorption is neglected.

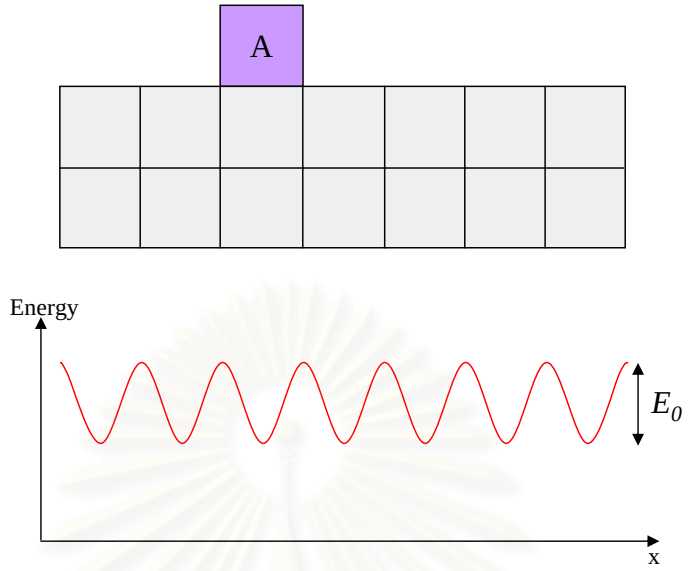

Figure 2.1: Schematic illustration of the lattice potential that diffusing atoms on flat surface must overcome to hop to the next neighboring site.

2.1.3 Surface Diffusion

After an atom reaches the growth front and forms bonds with other surface atoms in the deposition process, the atom can move on the crystal surface to search for the most stable position if it has enough energy to break its original bonds. To be more specific, in order for atom A in Fig. 2.1 to diffuse to a neighboring site on a flat surface, it must have enough energy to overcome a lattice potential that exists at the joint between lattice sites. The energy in this case is the thermal energy that atom A obtains from the substrate. Therefore, the hopping rate R, which is the number of hops in a unit time, increases with the substrate temperature T. The Arrhenius hopping rate is given by [9, 15, 16]

$$R = R_0 \exp(-\frac{E}{k_B T}), \tag{2.1}$$

where R_0 is a characteristic vibrational frequency, E is the activation energy, k_B is the Boltzmann constant, and T is the substrate temperature. The activation

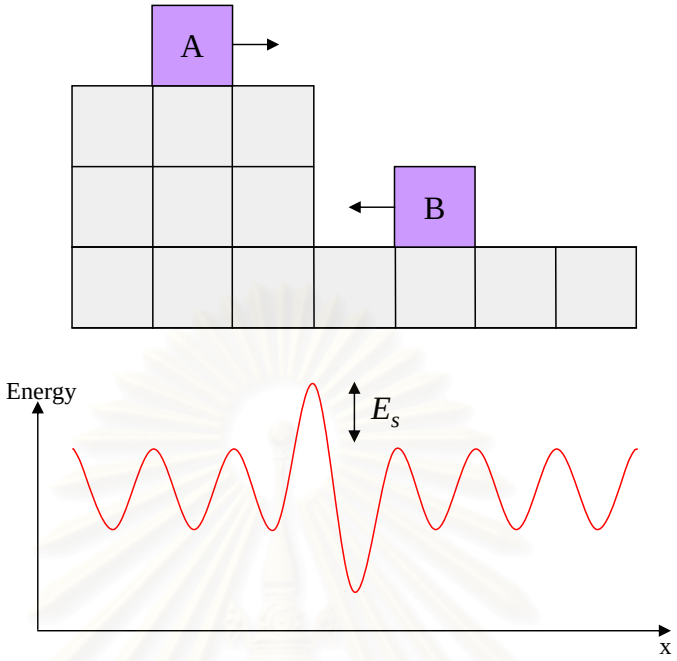

Figure 2.2: Schematic illustration of the additional potential barrier at the step edge, Ehrlich-schwoebel (ES) barrier, that diffusing atoms must overcome to hop down to the lower terrace.

energy is the amount of energy required for an atom with n lateral bonds to hop to a neighboring site. It is defined as $E = E_0 + nE_b$ where E_0 and E_b are the lattice potential and the lateral bonding energy per neighbor respectively. Therefore, an isolated atom, i.e. the atom without an lateral bond, can hop with higher hopping rate than the atom at a kink or pit site.

While diffusing across the growth front, atoms have a chance to encounter a step edge which is a region where two terraces of different height meet. When a diffusing atom approaches a step edge from the lower terrace such as atom B in Fig. 2.2, it preferentially sticks to that kink site at the bottom of the step edge. However, when a diffusing atom approaches a step edge from the upper terrace such as atom A in Fig. 2.2, it has been shown experimentally that the diffusing atom will preferentially stick to the edge of the upper terrace instead of hopping down to the lower terrace. This is because there is an additional potential barrier

at the step edge that a diffusing atom must overcome in order to be able to hop down [6, 7]. This barrier is known as the Ehrlich-Schwoebel (ES) barrier [6, 7]. We will discuss effects of the ES barrier on MBE growth in detail in Chapter 4.

2.2 Discrete Growth Models

Since the study of MBE growth by the use of computer simulations has attracted scientist's attention for years, a number of discrete growth models have been proposed to describe the kinetic roughening phenomena of the surface growth. Some of the well known discrete models are the random deposition (RD) model [13], the Das Sarma-Tamborenea (DT) model [17, 18], the Wolf-Villain (WV) model [19], and the MBE model [8, 9, 10]. For these discrete growth models, each atom is simplified to a simple unit square block and there is no off-lattice. In addition, a periodic boundary condition and the solid-on-solid (SOS) constraint [11, 20], where bulk vacancy, overhanging, and desorption are omitted, are applied. In this thesis, we focus on a 1+1 dimensional discrete growth model where the growth is performed on 1 dimensional substrate (d'=1) of size L.

In this section, the simplest version of discrete growth models called the RD model, where there is no diffusion, will be described first. Although it is the simplest model, results of this model agree well with the more complicated model, i.e. the MBE model, in some conditions. Then discrete models which include effects of the diffusion process, i.e. the DT model and the MBE model, will be discussed later in the section.

2.2.1 Random Deposition Model

The RD model includes only the deposition process while desorption and diffusion of atoms are not allowed. The site that an atom will be deposited on is randomly chosen. Then the atom falls vertically until it reaches the top of that site and be

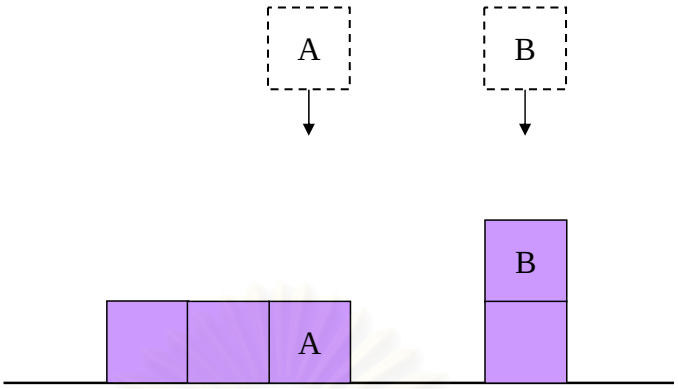

Figure 2.3: Schematic illustration of the RD model. Atoms fall vertically until they reach the top of the randomly selected site and stick irreversibly.

incorporated there permanently. (See atom A and B as illustrated in Fig. 2.3.) The characteristic of this model is that each lattice site is grown independently so there is no correlations between neighboring sites.

2.2.2 Das Sarma-Tamborenea Model

The DT model [17, 18] is a dynamical model that once an atom is deposited at a random site, it can diffuse immediately to a neighboring site according to the DT diffusion rules. In this model, only the freshly deposited atom can diffuse and once the atom hops to a neighboring site, it is incorporated there permanently. The DT diffusion rule requires atoms to hop to increase their coordination numbers, i.e. the number of bonds they form with their nearest neighbors. Atoms with at least one lateral bond, e.g. atom B and F in Fig. 2.4, do not move. If there are more than one site to hop to increase the coordination numbers at a moment, e.g. atom C and G, the diffusing atoms will choose a final site randomly. In addition, if there is no site with higher coordination number to hop to, e.g. atom E, then the diffusing atoms will be incorporated at their deposition site.

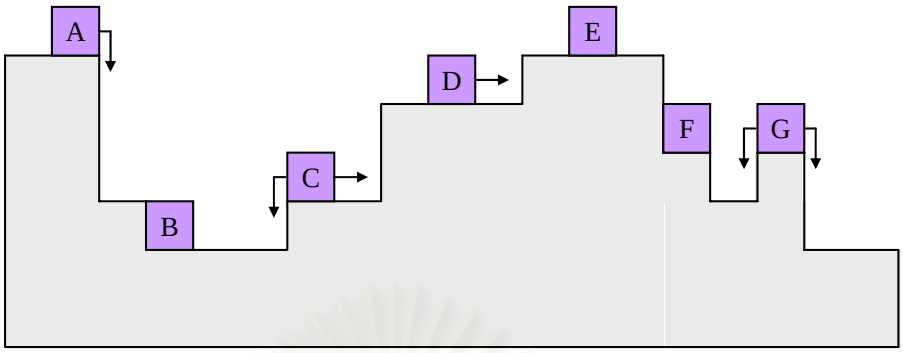

Figure 2.4: Schematic configuration defining the diffusion rules for the DT model.

2.2.3 MBE Model

The MBE model [8, 9, 10] was created as a realistic model to study MBE growth. In this model, desorption is neglected and only the deposition and diffusion processes are included similar to the DT model. However, in the MBE model, all atoms that are still on the surface of the growing film can hop. The hopping rate of each atom depends on the initial bonding configuration of that atom and the temperature of the substrate, which makes this model a comparatively realistic one.

In the MBE model, the deposition process is simulated by dropping one atom at a time on the substrate. Atoms are dropped to randomly selected sites with a constant deposition rate. During diffusion process, any surface atom (not only a freshly deposited one) can hop to a random neighboring site with hopping rate depending on the Arrhenius expression Eq. (2.1). The parameters used here are E_0=1.0 eV, and E_b= 0.3 eV unless noted otherwise. With these values of parameters and substrate temperature T=650 K, an atom on flat surface, i.e. an atom without any lateral bond, will hop approximately 200 times greater than an atom at a kink site, i.e. atom with one lateral bond. Therefore, once an atom sticks at a kink site, it will remain there for a long time. The hopping period τ, a period of time that an atom spends to complete a hop to a neighboring site, can

be calculated from $\tau = 1/R$.

Solid on solid (SOS) constraint is assumed in this study. The SOS constraint requires that a deposited atom will fall on top of a random column. Freshly deposited atoms typically do not immediately hop, but at this moment a hopping rate of every surface atom will be calculated. Then an atom which has a maximum hopping rate will be selected to hop. The SOS constraint forces it to hop from its position to the top of a neighboring column. We point out that the motion of the atom will affect the bonding configuration of the surface, so we must calculate the hopping rate of surface atoms again before selecting the next atom to hop [10].

2.3 Dynamical Scaling Hypothesis

In general, the aim of thin film growth is to obtain a high quality film, i.e. a smooth film, because it has good contact properties and is suitable for electronic devices. However, grown films are generally not absolutely smooth. Most of the time, there exists some roughness on surfaces of the films. This roughness is a result of kinetic roughening that occurs during growth process. The kinetic surface roughening phenomenon during thin film growth is what we want to understand. To study this problem quantitatively, we can use the interface width W [13], which is a root mean square height fluctuation of a growing surface:

$$W(L,t) = \left\langle (h - \langle h \rangle)^2 \right\rangle^{1/2}, \tag{2.2}$$

where $h \equiv h(x,t)$ is the surface height at substrate site x and time t, $\langle h \rangle$ is the average height, L is the size of the substrate, and $\langle ... \rangle$ means that the quantity in that bracket is averaged over the substrate. According to dynamical scaling hypothesis, the interface width scales with L and t as [21, 22]

$$W(L,t) \sim L^{\alpha} f(L/\xi(t)), \tag{2.3}$$

where L is the substrate size, α is the roughness exponent, and $f(y)$ is the scaling function which follows:

$$f(y) \sim \begin{cases} const & \text{for } y \ll 1 \\ y^{-\alpha} & \text{for } y \gg 1. \end{cases} \tag{2.4}$$

Here $\xi(t)$ is the lateral correlation length, which obeys the dynamical scaling behavior,

$$\xi(t) \sim \begin{cases} t^{1/z} & \text{for } t^{1/z} \ll L \\ L & \text{for } t^{1/z} \gg L, \end{cases} \tag{2.5}$$

where z is the dynamical exponent. Combining Eqs. (2.3) - (2.5), scaling behavior of the interface width is obtained,

$$W(L,t) \sim \begin{cases} t^{\beta} & \text{for } t \ll L^z \\ L^{\alpha} & \text{for } t \gg L^z, \end{cases} \tag{2.6}$$

where $\beta = \alpha/z$ is the growth exponent. For a system with a constant substrate size L, the interface width initially increases as a power law in time, and then saturates at asymptotic time ($t \gg L^z$). The growth exponent can be obtained from the slope of the plot of the interface width as a function of time. Since the slope must be calculated from data in the $t \ll L^z$ range, the substrate size L should be large enough in order to have enough data for an accurate β calculation.

The interface width is calculated from height fluctuations measured with respect to the globally averaged height, so it describes the global scaling behavior. However, we can study the local scaling behavior by studying the height difference correlation function,

$$G(r,t) = \left\langle |h(x+r,t) - h(x,t)|^2 \right\rangle^{1/2}, \tag{2.7}$$

where r is a distance between two sites on the substrate and $\langle ... \rangle$ means that the quantity in that bracket is averaged over the substrate.

It is important to note that if the roughness exponent α is less than unity ($\alpha < 1$), the surface is self-affine and global and local properties of the system scale in the same manner. However, for $\alpha > 1$ or the so-called super rough surface, the global and local properties scale differently.

For self-affine surfaces ($\alpha < 1$), the conventional scaling form of the height difference correlation function is

$$G(r,t) \sim r^{\alpha} g(r/\xi(t)), \tag{2.8}$$

where $g(y)$ is the same as the scaling function $f(y)$ in Eq. (2.4). However, for super rough surfaces ($\alpha > 1$), there is anomalous dynamical scaling that global and local properties of system scale differently. The scaling function $g(y)$ in Eq. (2.8) is not the same as $f(y)$ in Eq. (2.4), but follows

$$g(y) \sim \begin{cases} y^{-\kappa/2} & \text{for } y \ll 1 \\ y^{-\alpha} & \text{for } y \gg 1. \end{cases} \tag{2.9}$$

When the length scale is greater than the correlation length ($r \gg \xi(t)$), the scaling function is not different from the self-affine scaling discussed previously. However, it is quite different when the length scale is less than the correlation length ($r \ll \xi(t)$).

Combining Eq. (2.8) and Eq. (2.9), we obtain the asymptotic behavior of $G(r,t)$ for super rough surfaces:

$$G(r,t) \sim \begin{cases} r^{\alpha-\kappa/2} t^{\kappa/2z} & \text{for } r \ll t^{1/z} \ll L \\ r^{\alpha-\kappa/2} L^{\kappa/2} & \text{for } r \ll L \ll t^{1/z} \\ t^{\beta} & \text{for } r \gg t^{1/z}. \end{cases} \tag{2.10}$$

The additional scaling exponent κ is equal to zero for self-affine surfaces. Therefore, Eq. (2.10) can be written as

$$G(r,t) \sim \begin{cases} r^{\alpha} & \text{for } r \ll t^{1/z} \\ t^{\beta} & \text{for } r \gg t^{1/z}. \end{cases} \tag{2.11}$$

It is consistent with Eq. (2.6), which is the behavior of global scaling.

For self-affine surfaces, the roughness exponent α can be obtained by measuring the slope from $G(r,t)$ versus r log-log plot at small r. However, for super rough surfaces, the slope of that plot changes from α to $\alpha' = \alpha - \kappa/2$, so we cannot find α by this method. The well-known method to find α in a super rough surface is to perform a scaling collapse by plotting $G(r,t)/r^{\alpha}$ versus $r/t^{1/z}$ for several sets of data at various time and changing the value of α and z until all data collapse onto one line.

Chapter 3

MBE Growth

Using the MBE model to simulate molecular beam epitaxy growth, our simulation results are presented in this chapter. Surface morphologies at various substrate temperatures and scaling properties of the model are shown. We also present a relation between the surface diffusion length and the substrate temperature (which is a controllable parameter in real experiments) in the last section.

3.1 Morphologies

In this section, simulation results of surface morphologies at various substrate temperatures (T) are presented. In Fig. 3.1 snapshots of surface morphologies at T=450, 500, 550, 650, and 750 K are shown (bottom to top). All data are from systems of substrate size L=1000 lattice sites and the morphologies are at 1000 MLs (monolayers) thickness. It is obvious from Fig. 3.1 that at low T, i.e. 450 K, the surface is very rough and it becomes smoother when T increases.

We can divide these temperature-dependent morphologies into three main regimes. The first regime is at low T, at approximately 450 K. In this regime surface diffusion is very rare and atoms stick where they first arrive on the growing surface most of the time. The second regime is at intermediate T where surface diffusion has more effect on the growth process. Consequently, morphologies from this intermediate regime are smoother than ones at low T regime. It should be

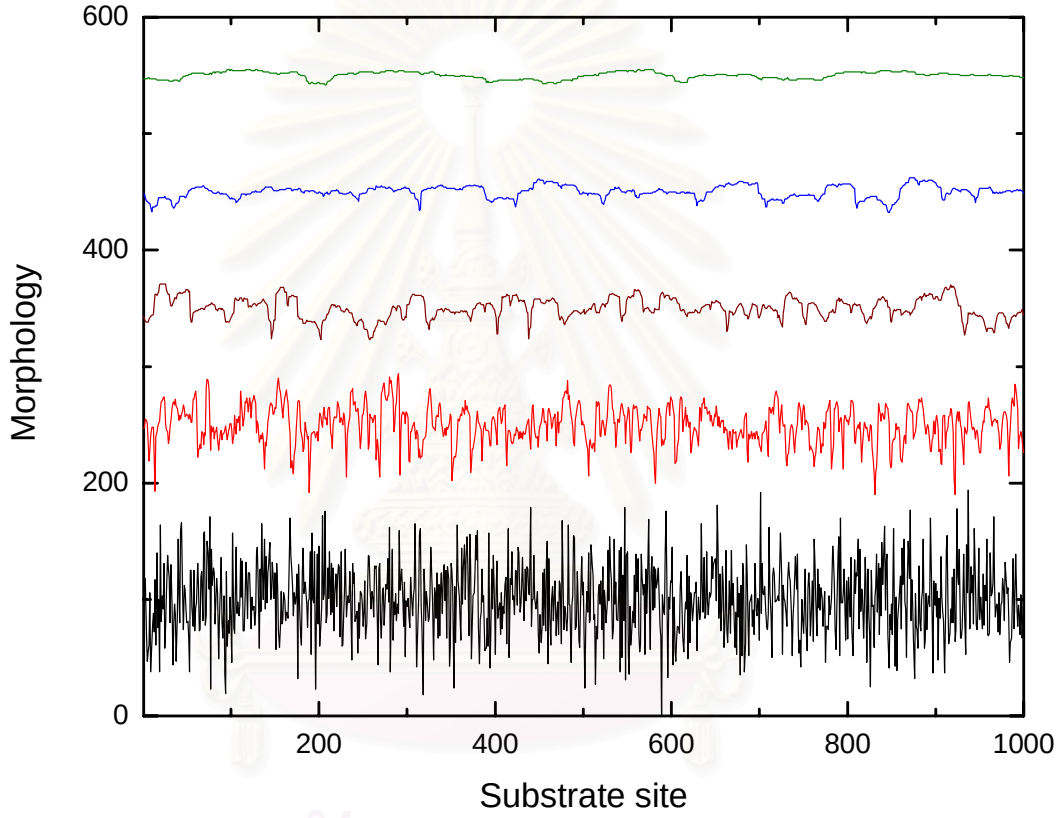

Figure 3.1: Surface morphology of the MBE model at T=450, 500, 550, 650, and 750 K (bottom to top) for system of L=1000 and t=100 MLs.

noted, however, that these intermediate T morphologies are still kinetically rough surfaces. The third regime is at high T where atoms have long surface diffusion length. Therefore, they can search for an energetically favorable position, i.e. kink or pit, to stick. As a result the surfaces become extremely smooth as the growth process becomes a layer-by-layer growth.

We found that at some T, the morphology of the MBE model is statistically equivalent to that of other dynamical models described in the previous chapter. For example, in Fig. 3.2 the surface morphology of the MBE model at T=450 K is very similar to that of the RD model, which omits surface diffusion of atoms. And in Fig. 3.3 the surface morphology of the MBE model at T=550 K shows deep grooves with relatively flat tops which looks like results of the DT model.

3.2 Scaling

In order to study scaling properties of the MBE model, we first start with the interface width (global scaling). In Fig. 3.4, interface widths of systems at substrate temperature T= 450, 500, 550, 600, 650, 700, 750, and 800 K are plotted as a function of time in log-log scale (top to bottom). The effective growth exponents β_{eff} of each T are extracted from slopes of these plots and shown in Fig. 3.5. We found that at 450 K, β_{eff} is equal to 0.5. It is the same as the RD model, where diffusion is not allowed at all. It is important to note that in the RD model β is equal to 0.5 while α and z approach infinity. The similarity of the growth exponents confirms the consistence between the MBE model at low T and the RD model. As T increases, β_{eff} decreases from 0.5. It is also interesting that at high T, i.e. 750 and 800 K, we can see oscillations of the interface width during early time. The oscillation corresponds to layer-by-layer growth in the first few layers. The layer-by-layer growth means that films will be grown completely in a layer before the next upper layer starts being grown.

It is not sufficient to study scaling properties by using only the growth expo-

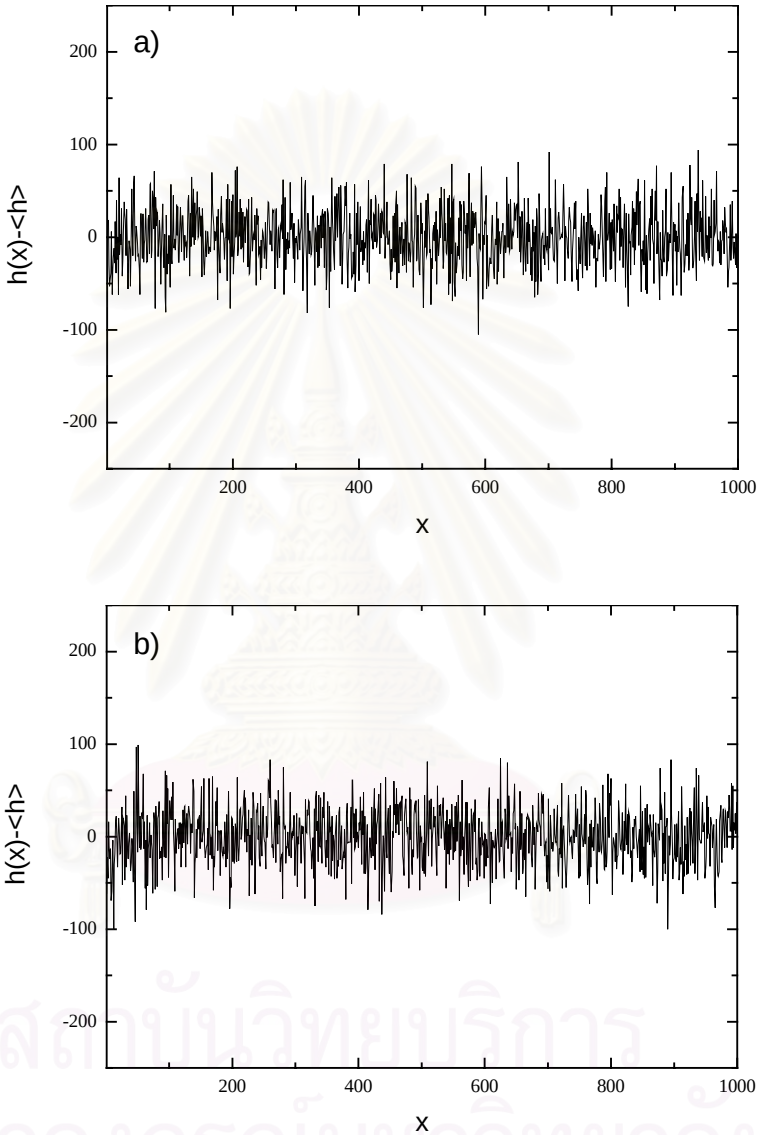

Figure 3.2: The comparison of surface morphology between a) the MBE model at 450 K and b) the RD model

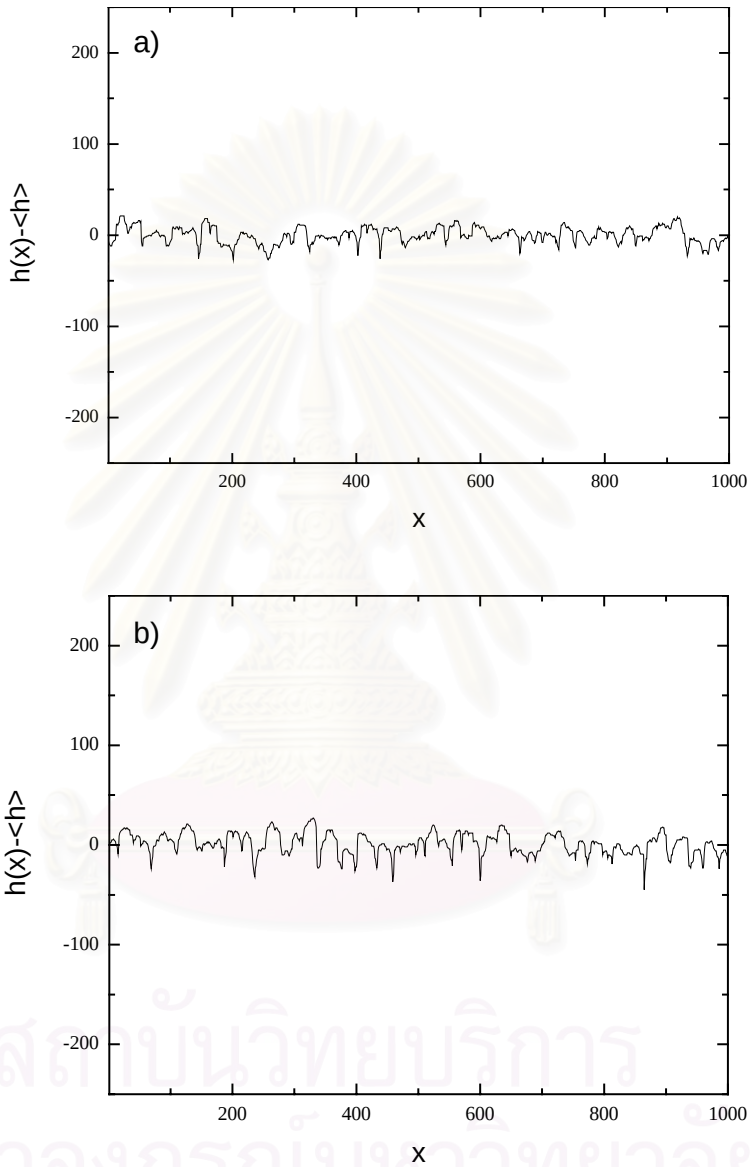

Figure 3.3: The comparison of surface morphology between a) the MBE model at 550 K and b) the DT model [23]

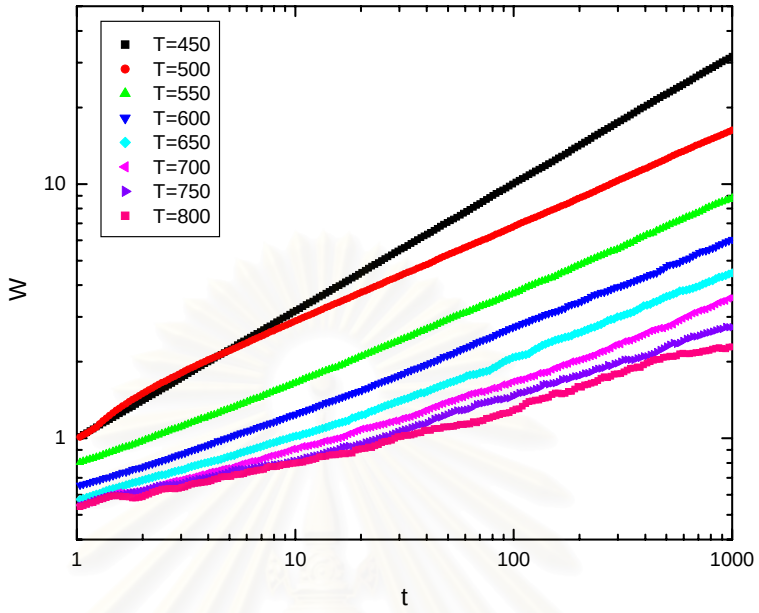

Figure 3.4: The interface width as a function of time of the MBE model at T=450, 500, 550, 600, 650, 700, 750 and 850 K. (top to bottom)

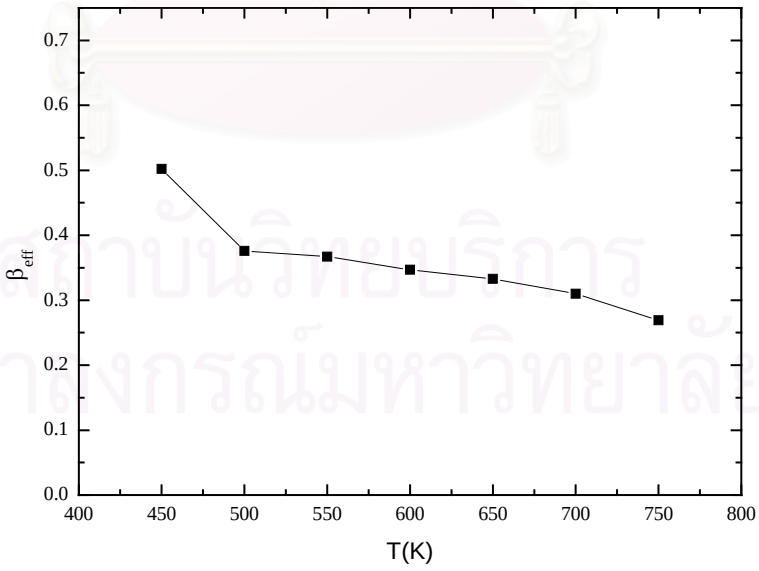

Figure 3.5: The effective growth exponent calculated from Fig. 3.4.

T (K)	α	β	z
600	1.16	0.374	3.10
650	1.10	0.364	3.02

Table 3.1: The critical exponents extracted from the data collapses in Fig. 3.6 and 3.7

nent. Here, we show a method to find other exponents, i.e. α and z, by performing data collapse. Figures 3.6 and 3.7 illustrate data collapses of 7 sets of data at different times between 2048 and 10^5 MLs at T=600 and 650 K respectively. The maximum time carrying on simulations is believed to approach the asymptotic time of the MBE model. The values of α and β are estimated from these plots by changing α and β to obtain the best fit of 7 sets of data and they are shown in Table 3.1. At both temperatures α is greater than unity. It implies that the MBE model at this intermediate temperature regime generates super rough surfaces. The specific characteristic of super rough surfaces is that they possess anomalous scaling behavior, i.e. global and local properties of the system are scaled differently.

To confirm the existence of anomalous scaling in the model, we also studied local scaling by plotting the height difference correlation function $G(r,t)$ as a function of r. From Eq. (2.10), when $r \ll t^{1/z}$ the slope of this plot is the local roughness exponent α'. If α' (local scaling) is not equal to α (global scaling), we can confirm the existence of the anomalous scaling of the model. In Fig. 3.8 $G(r)$ plots of substrate size L=1000 at time t=32768 MLs at T=600 and 650 K as a function of r are illustrated. The local roughness exponent α' from these plots is 0.69 and 0.67 for T=600 and 650 K respectively. The results show that global and local scaling are different ($\alpha \neq \alpha'$). Therefore, it confirms the existence of the anomalous scaling.

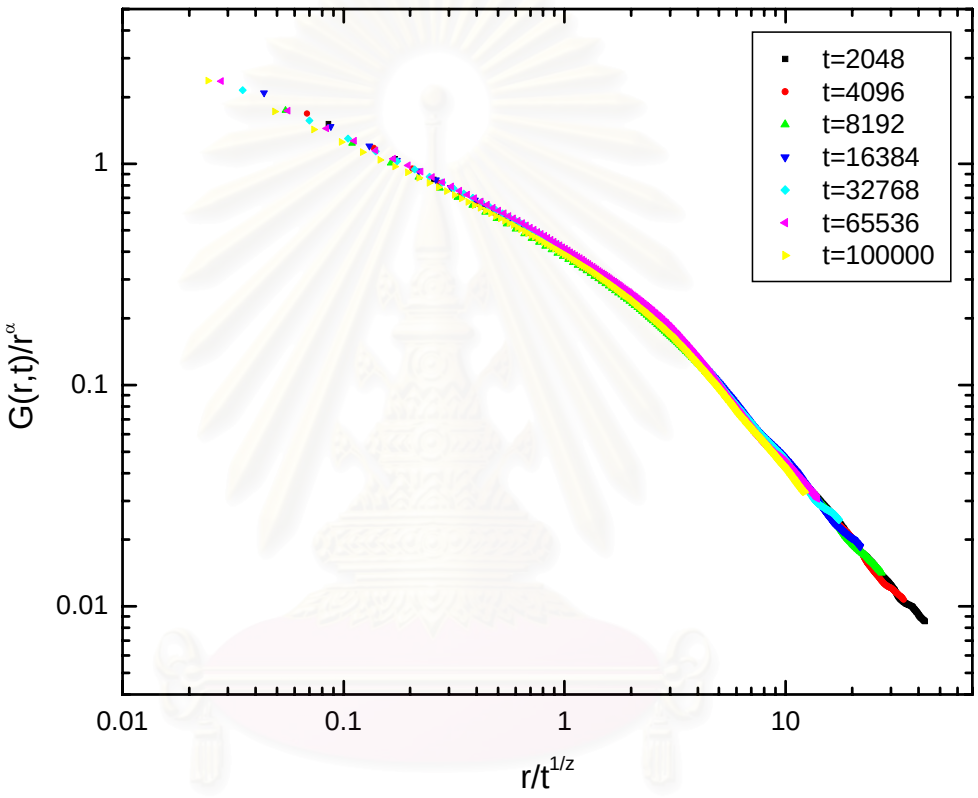

Figure 3.6: The data collapse of the MBE model at T=600 K for system of L=1000 and t=2048, 4096, 8192, 16384, 32768 and 10^5 MLs. The exponents from the best collapse are α =1.16, z=3.10 and consequently β=α/z = 0.374.

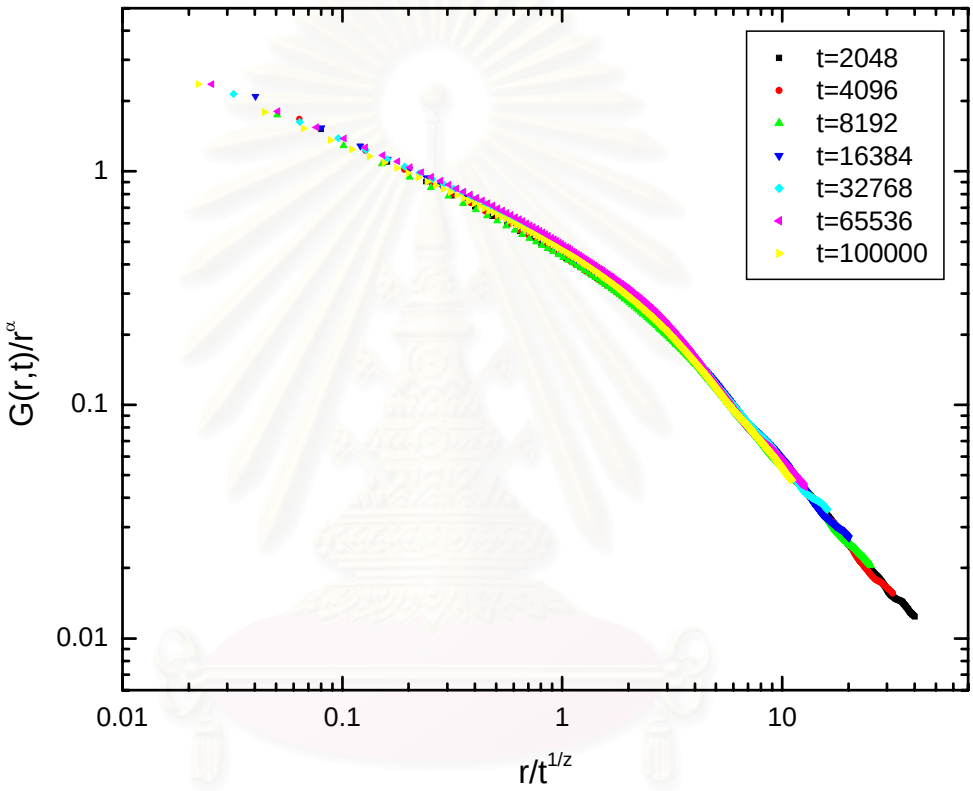

Figure 3.7: The data collapse of the MBE model at T=650 K for system of L=1000 and t=2048, 4096, 8192, 16384, 32768 and 10^5 MLs. The exponents from the best collapse are α =1.10, z=3.02 and consequently β=α/z = 0.364.

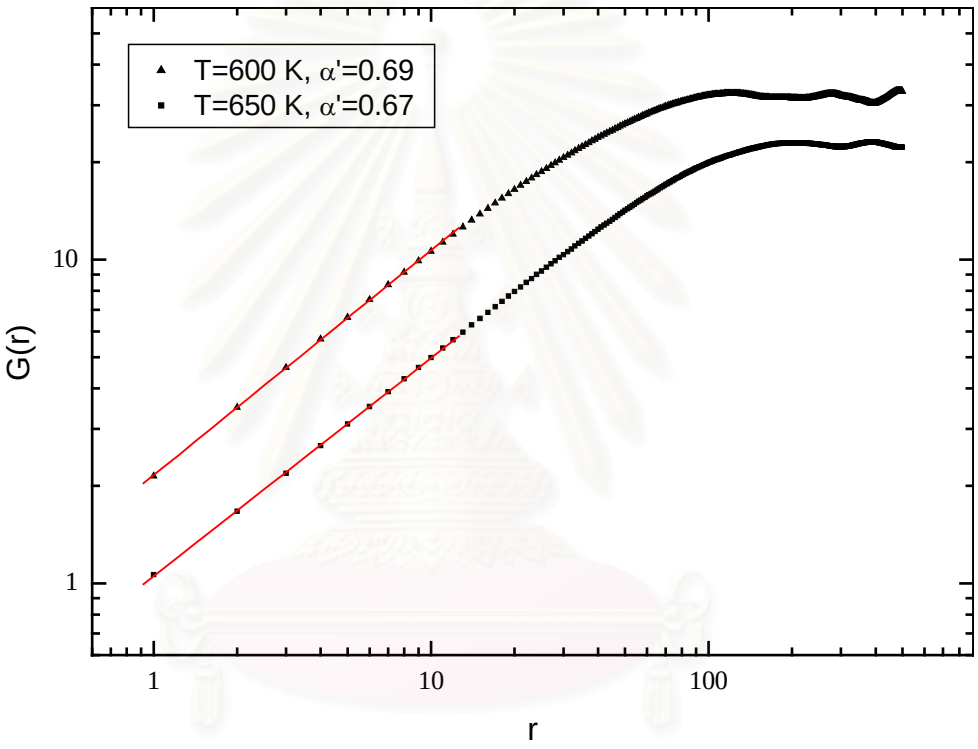

Figure 3.8: The $G(r)$ plot from substrate size L=1000 at time t=32768 MLs for T=600 and 650 K.

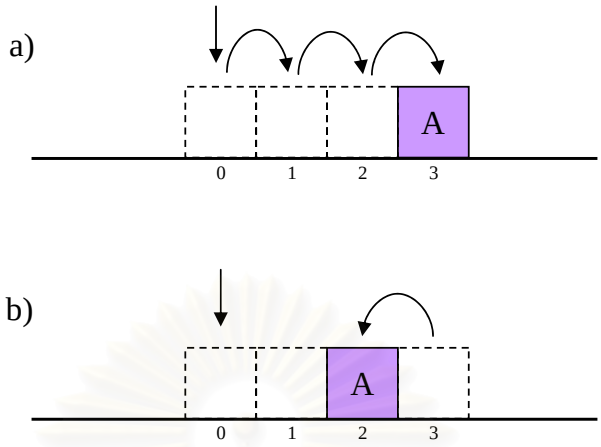

Figure 3.9: Schematic illustration of the surface diffusion length calculation used in the simulations

3.3 Surface Diffusion Length

In MBE growth, an atom deposited on the substrate tries to diffuse to an appropriate site before being incorporated. The displacement that a freshly deposited atom can diffuse before being incorporated into a growing film is called the surface diffusion length ℓ_d. The surface diffusion length is one of the important parameters that have effects on the film quality. In this section, a relation between the surface diffusion length ℓ_d and the substrate temperature T is presented. This relation is of interest because T is a controllable parameter in real experiments.

In computer simulations based on the MBE model, ℓ_d is determined by keeping track of each freshly deposited atom until it is incorporated and becomes a part of the substrate. For example, atom A in Fig. 3.9 a) is initially deposited on the substrate at position 0 and then hops three times to position 3. At this moment, the surface diffusion length is equal to three. Afterwards, if atom A hops back to the left neighboring site as illustrated in Fig. 3.9 b), now the surface diffusion length reduces to two. In simulations, atom A will be monitored until it is incorporated permanently into the film and the distance between the final

position and the original position of atom A is the surface diffusion length of atom A. Every freshly deposited atom is monitored this way and the average of the diffusion length of all atoms becomes the surface diffusion length ℓ_d of the system at that value of the substrate temperature T.

Our results of ℓ_d as a function of T at deposition rate F=0.1, 1, and 2 ML/s are shown in Fig. 3.10 (top to bottom). For each deposition rate, we find that ℓ_d increases with increasing T as $\ell_d \propto e^{-A/T}$. Consequently, surface morphologies become smoother when T is higher, because atoms can search further away from their original deposition sites for the most energetically favorable positions. At the same T, atoms deposited with high deposition rate F will possess a smaller ℓ_d than ones deposited with lower F. This is because with the high deposition rate, new atoms are deposited quickly on the substrate. This increases a chance that a surface atom will be "buried" underneath newly deposited atoms and then lost its ability to diffuse. In other words, the period of time that an atom remains "active" is shorter in a system with higher deposition rate resulting in smaller surface diffusion length in the system. Note that when T is low enough, ℓ_d will fall all the way down to zero. It means that atoms cannot diffuse at all during growth process so they will stick where they first arrive on the growing surface. As a result, the surface morphologies become very rough as we have seen in the previous section. In this very low T regime, the MBE model is very similar to the simple RD model. We have found that the value of this "cut-off" T (when there is no diffusion on the surface) varies with the deposition rate as well.

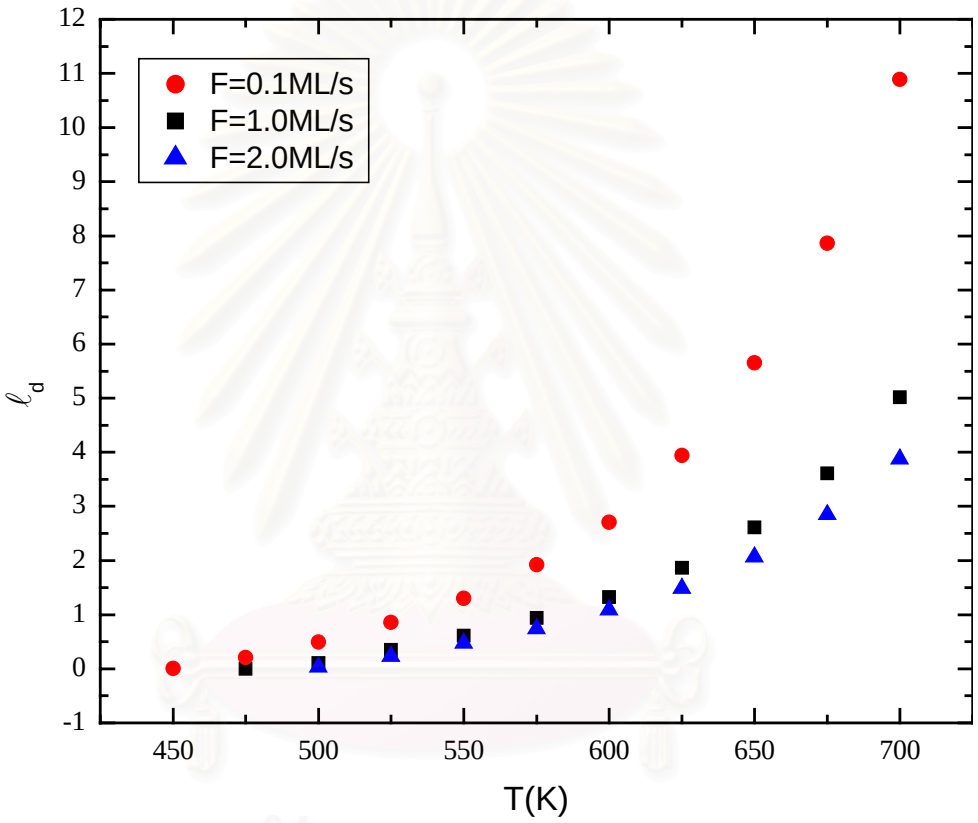

Figure 3.10: The relations between ℓ_d and T for the systems with F=0.1, 1, and 2 ML/s.

Chapter 4

ES Barrier in MBE Growth

After having studied the molecular beam epitaxy growth in systems without the Ehrlich-Schwoebel barrier in the previous chapter, we will present our simulation results of MBE growth under the ES effects in this chapter. Since ES barrier causes mound formation, we studied mound properties, i.e. the average mound radius and the average mound height, by using the height-height correlation function. Observing the mound radius and the mound height evolution, we found that the MBE model with ES barriers and the RD model, although not the same, share a few similar characters.

4.1 MBE Model with ES Barrier

In order to study effects of the Ehrlich-Schwoebel barrier on MBE growth, the basic MBE model will be modified. Since the ES barrier occurs at the edge between two terraces of different height, diffusing atoms must overcome this additional barrier to hop to another terrace. It means that an atom will encounter the ES barrier if it tries to hop to another site with different height. If it does not have enough energy to overcome this barrier, it has to stay at its original site. For example, if atom A in Fig. 4.1 tries to hop down to the lower terrace on its left side (the site with smaller height), it will encounter the ES barrier. On the contrary, if atom A tries to hop to the neighboring site on the right, the ES barrier will have no effect on it. The probability that diffusing atoms successfully hop to another

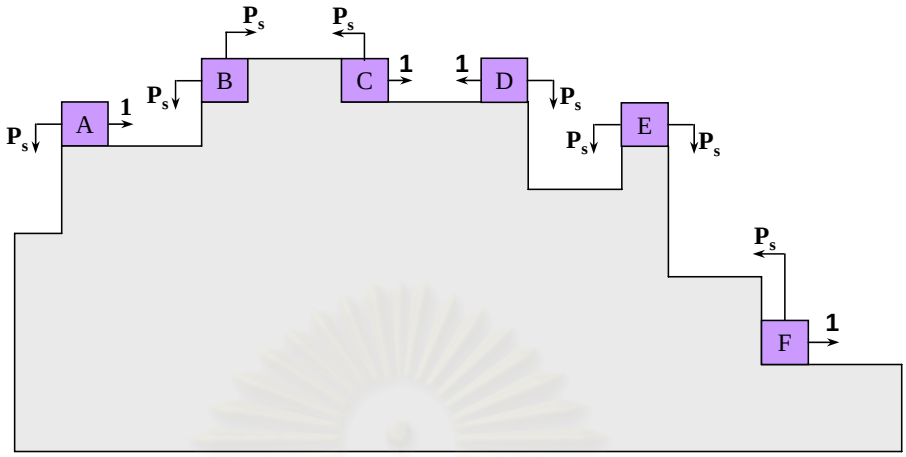

Figure 4.1: The effects of ES barrier on diffusion behavior of diffusing atoms. A diffusing atom will encounter the ES barrier if it try to hop to the site with different height (direction marked P_s on arrowhead). However, it does not encounter the barrier if it hop to the site with equal height (direction marked 1 on arrowhead).

site is defined by the *tunneling probability*,

$$P = \begin{cases} P_s = e^{-E_s/kT} & \text{for } \Delta h \neq 0 \\ 1 & \text{for } \Delta h = 0, \end{cases} \tag{4.1}$$

where E_s is the strength of the ES barrier, T is the substrate temperature, and $\Delta h = h_f - h_i$ where h_f is the height after hopping and h_i is the height before hopping. From Eq. (4.1), it can be seen clearly that the probability that diffusing atoms can hop successfully is reduced greatly when they encounter ES barriers. The exact reduction depends on the strength of ES barriers, i.e. the probability to hop is very low when the ES barrier is very strong. In addition, the hopping rate of diffusing atoms under effects of the ES barrier is changed to

$$R_{ES} = P \cdot R, \tag{4.2}$$

where R is the original Arrhenius hopping rate defined in Chapter 2. From the

above equations, the hopping rate of diffusing atoms that encounter the barrier is reduced with the factor P_s whereas the hopping rate of diffusing atoms that do not encounter the barrier stay at the same value of the original Arrhenius hopping rate.

4.2 Morphologies

In this section, time evolution of surface morphologies under the effects of the ES barrier is presented. The strength of the barrier is defined via the tunneling probability P described in the previous section. In Fig. 4.2, surface morphologies under effects of a moderate barrier are shown. The tunneling probability in this system is P_s=0.5 which is equivalent to E_s=0.039 eV and the substrate temperature is fixed at T =650 K. The morphologies here are at t=10^2, 10^3, 10^4 and 10^5 MLs (bottom to top) while the last one on the top line is from a system that does not include effects of ES barrier, i.e. P_s=1.0. Comparing surface morphologies under effects of ES barriers with the one that does not include the barrier, we can conclude that the ES barrier causes mound formations in the film surfaces. And we note that each mound can coarsen together during growth. Increasing the strength of ES barriers by changing P_s to 0.25 and 0.1 in the simulations, the results are shown in Figs. 4.3 and 4.4. Mound structures still occur; however, obviously, when the strength of ES barriers increases, the narrower and higher mounds are obtained. We also study growth at low barrier (large P_s) and find that mound structures coarsen with higher rate than that of higher barrier.

To study the effects of the substrate temperature on mound properties, we fix the strength of the barrier to P_s=0.5 and 0.1 and then carry out simulations at T=600, 650 and 700 K. Surface morphologies from P_s=0.5 at t=10^5 MLs at T=600, 650 and 700 K are plotted (bottom to top) in Fig. 4.5. The same thing from P_s=0.1 is illustrated in Fig. 4.6. Our results show that at moderate barrier (P_s=0.5) mound structures become wider and lower when T increases. Since at

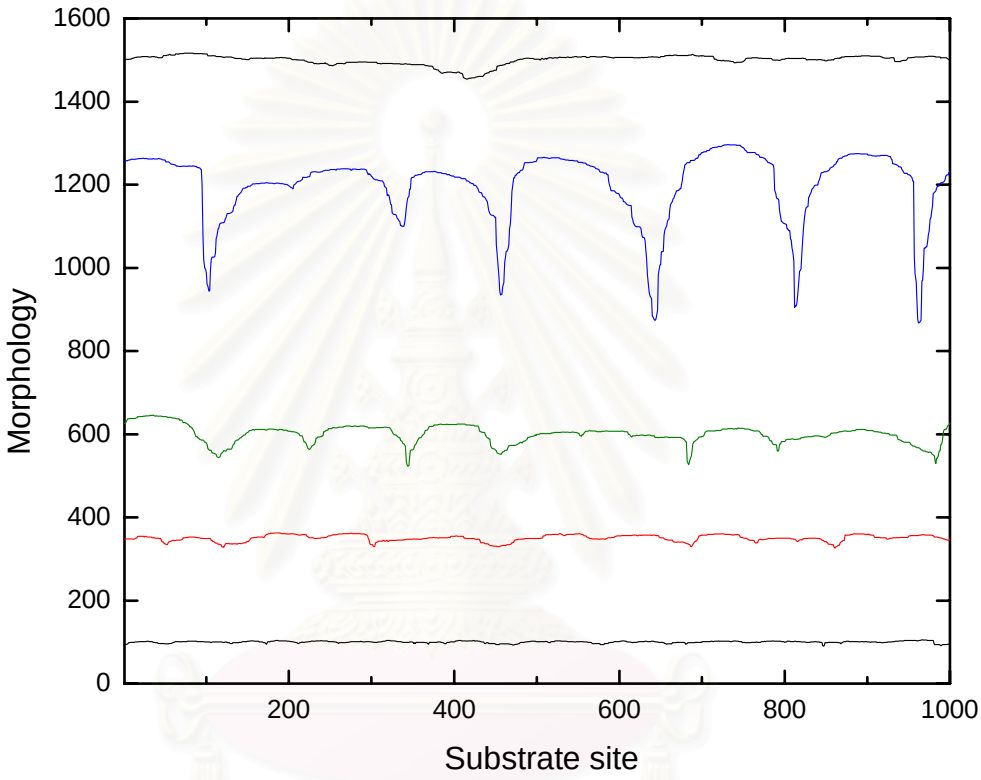

Figure 4.2: The mound evolution in the system with ES barriers for P_s=0.5 and T=650 K. Each line (bottom to top) presents the snapshot of surface morphology at t=10^2, 10^3, 10^4, 10^5 MLs. The top line is the snapshot of surface morphology of system without ES barrier (P_s=1.0)

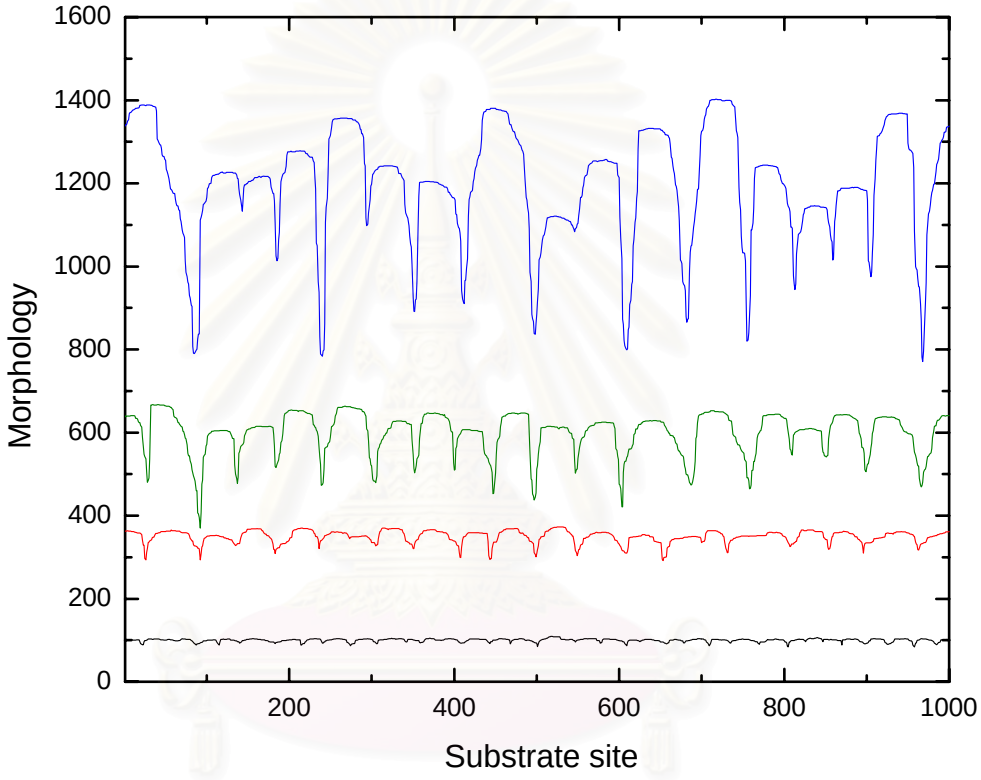

Figure 4.3: The mound evolution in the system with ES barriers for P_s=0.25 and T=650 K. Each line (bottom to top) presents the snapshot of surface morphology at t=10^2, 10^3, 10^4, 10^5 MLs.

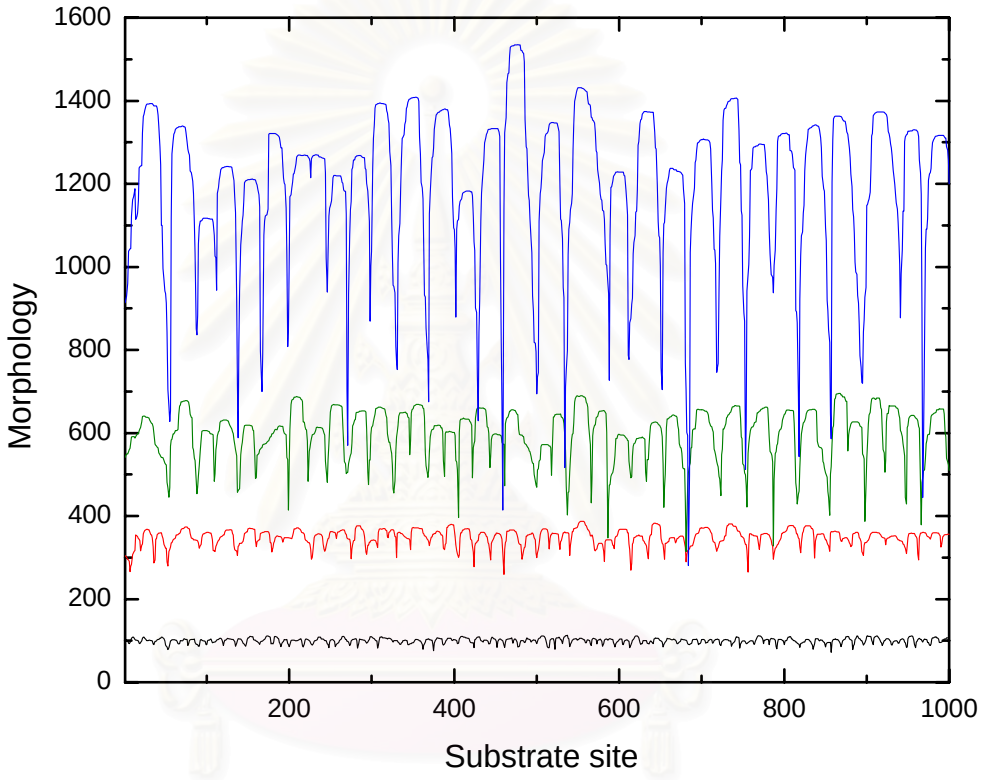

Figure 4.4: The mound evolution in the system with ES barriers for P_s=0.1 and T=650 K. Each line (bottom to top) presents the snapshot of surface morphology at t=10^2, 10^3, 10^4, 10^5 MLs.

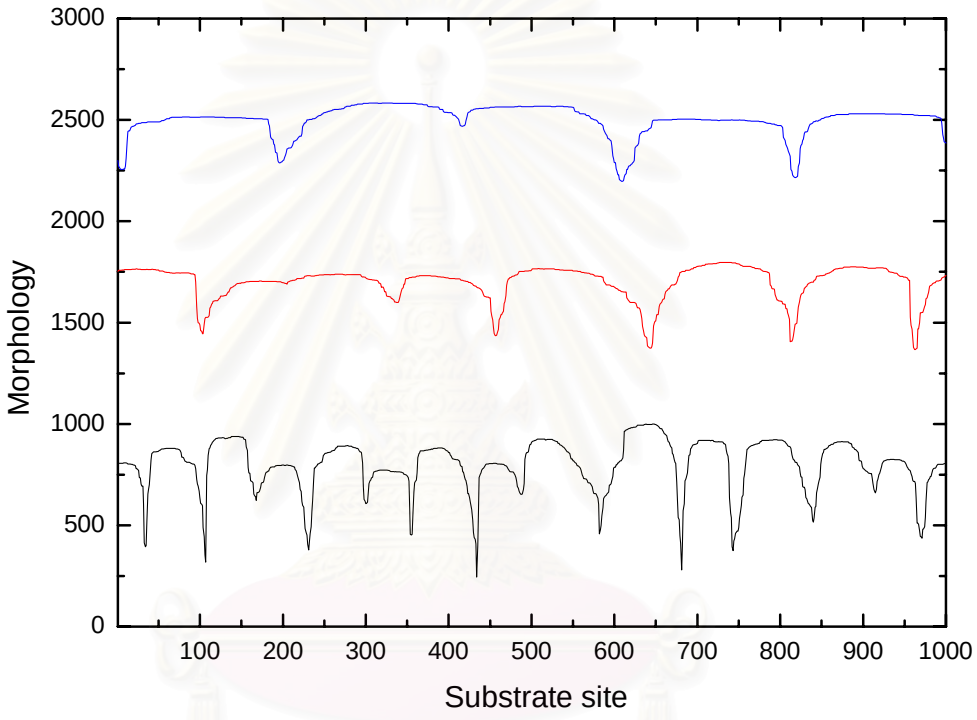

Figure 4.5: The effect of substrate temperature on mound shape. The snapshots present the surface morphologies of systems with moderate barrier (P_s=0.5) at t=10^5 MLs and T=600, 650, and 700 K (top to bottom).

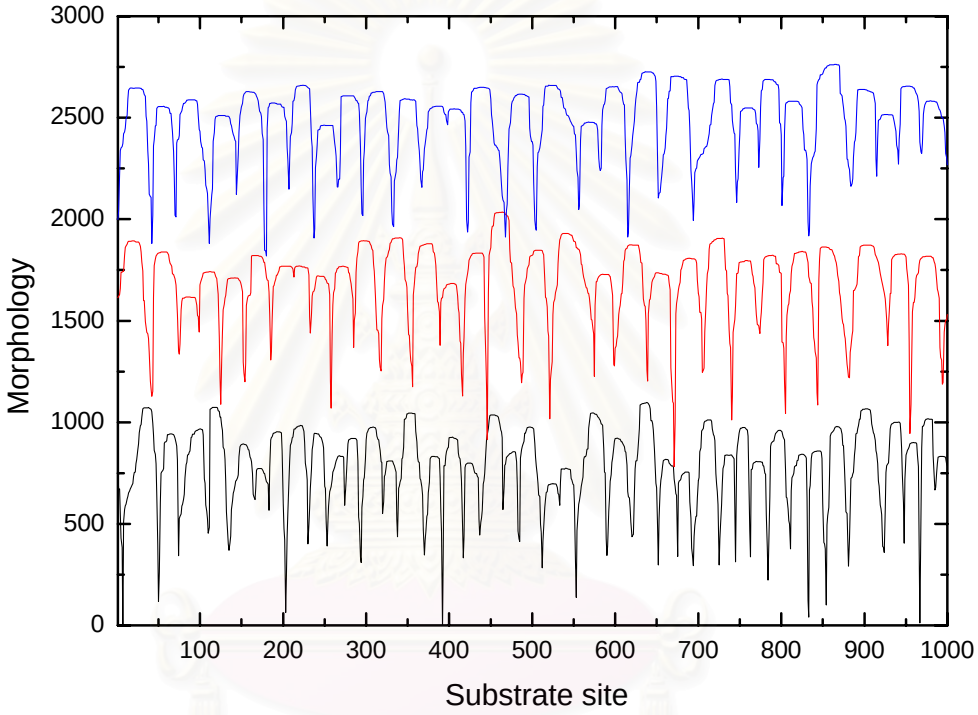

Figure 4.6: The effect of substrate temperature on mound shape. The snapshots present the surface morphologies of systems with strong barrier (P_s=0.1) at t=10^5 MLs and T=600, 650, and 700 K (top to bottom).

high T diffusing atoms have enough energy to overcome the barrier, they can hop down to fill up grooves so the individual mound can coarsen together resulting in a wider and lower mound structure. However, at high barrier (P_s=0.1), increasing T in the same range does not have much effects on mound properties. Since the strength of the barrier is so high that only few diffusing atoms can hop down to fill up the groove in this range of substrate temperature, each mound hardly coarsens resulting in small change in the structure.

To study mound properties in more details, the function $H(r)$ [11, 12] is used. This height-height correlation function is defined [11, 12] as

$$H(r) =< h(\mathbf{x})h(\mathbf{x}+\mathbf{r}) >_x , \tag{4.3}$$

where $r = |\mathbf{r}|$ is the distance between two sites on the substrate and $\langle ... \rangle_x$ means the quantity is averaged along the substrate. The specific feature of this correlation function is that for surfaces with mound pattern $H(r)$ will oscillate around $H = 0$ line as illustrated in Fig. 4.7. The average mound radius can be obtained from the distance of the first zero-crossing of this plot. In addition, the average mound height is calculated from $[H(r = 0)]^{1/2}$.

In Fig. 4.8 a), the mound radii calculated from $H(r)$ plots at T=600 (square), 650 (circle) and 700 K (triangle) for P_s=0.1 (filled symbol) and 0.5 (open symbol) are plotted as a function of t. For each line, the mound radius initially increases rapidly and then saturates at some value. This shows that at initial time, small mounds coarsen together resulting in bigger mounds, or in other words, increasing of mound radius. The coarsening process goes on continuously until the system reaches a saturate regime where the coarsening process is extremely slow resulting in the almost-constant mound radius.

We found that the values of these saturated radii depend on both the substrate temperature and the strength of the ES barrier. The saturated radius

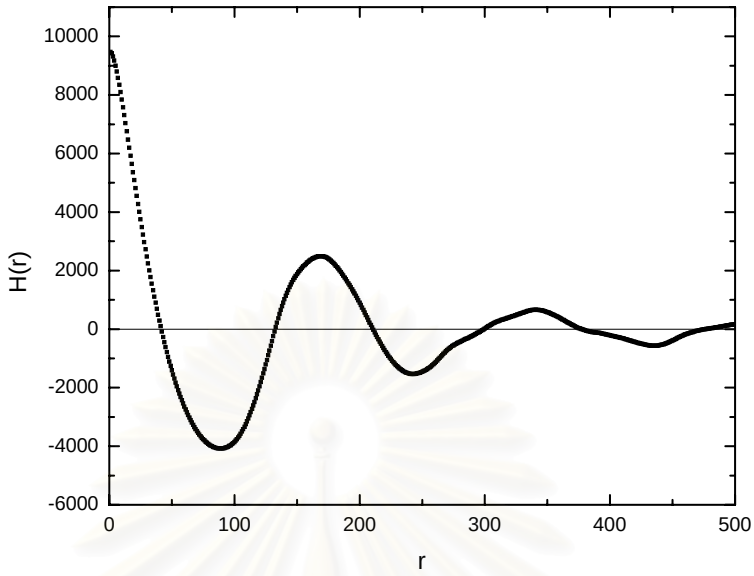

Figure 4.7: The height-height correlation function $H(r)$ as a function of r from the system with ES barriers. Parameters used here are T=650 K, L=1000, P_s=0.5, and t=10^5 MLs

increases when T increases, especially for a system with low barrier that increasing T has more effects on the saturated radius than a system with high barrier. Since in the system with high T individual mound coarsens faster than that in the system with lower T, after coarsening regime the saturated mound radius of a system with high T is certainly greater than that of a system with lower T.

At each T, the saturated mound radius of a system with low barrier, i.e. P_s=0.5, is obviously greater than one with higher barrier, i.e. P_s=0.1. We can say that for P_s=0.1 the barrier is so strong that there is very few diffusing atoms that can overcome this barrier and hop to the groove as part of the coarsening process. As a result, the rate of coarsening is very slow. Since in the system with high barrier individual mound coarsens slower than the system with lower barrier, after coarsening regime the saturated mound radius of a system with high barrier is certainly smaller than that of a system with lower barrier. In Fig. 4.9 a), the evolution of mound height is presented. For each line, the mound height

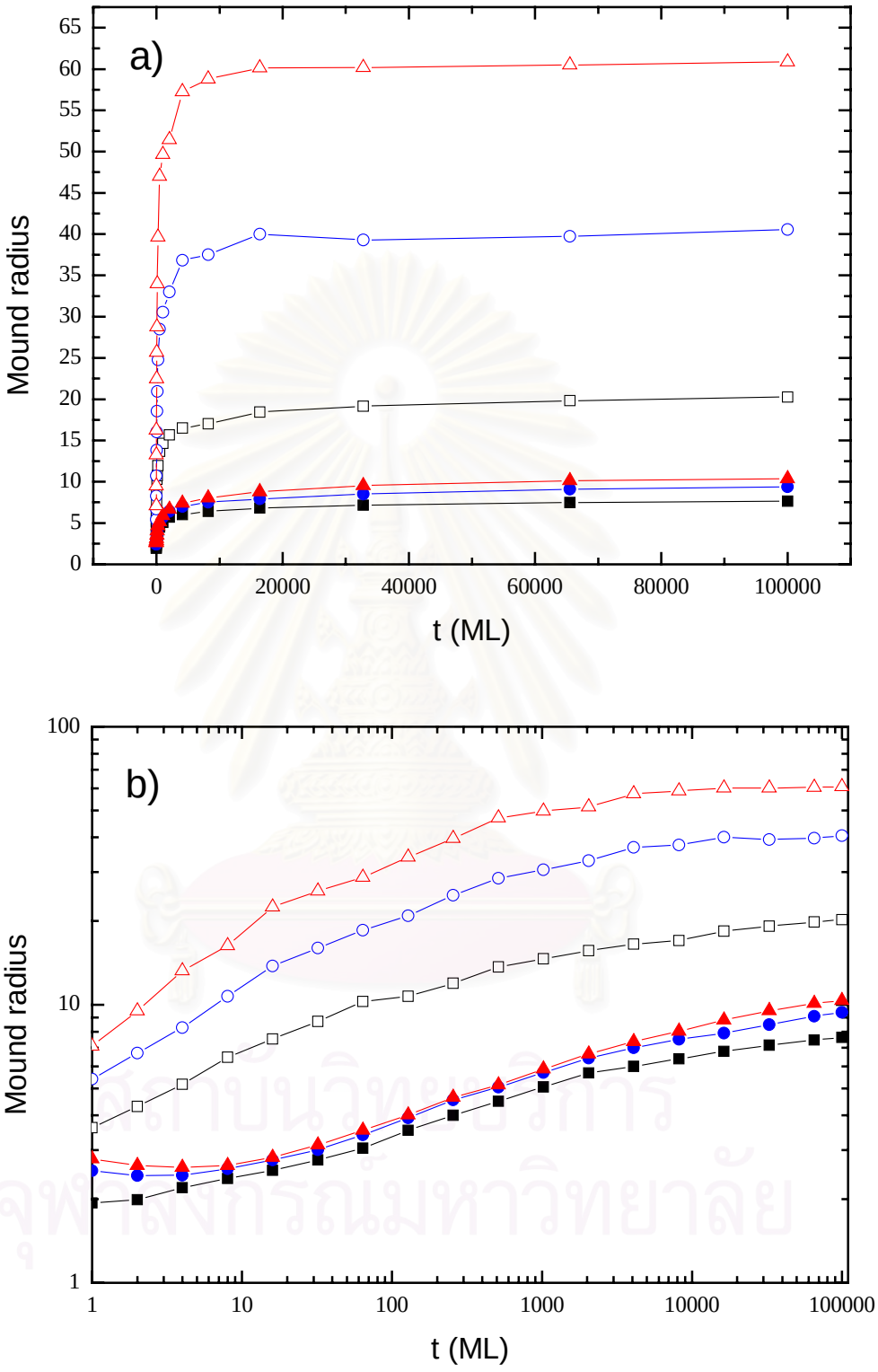

Figure 4.8: The evolution of the average mound radius of the system with P_s=0.1 (filled symbol) and 0.5 (open symbol) at T=600 (square), 650 (circle), and 700 K (triangle). a) normal scale b) log-log scale

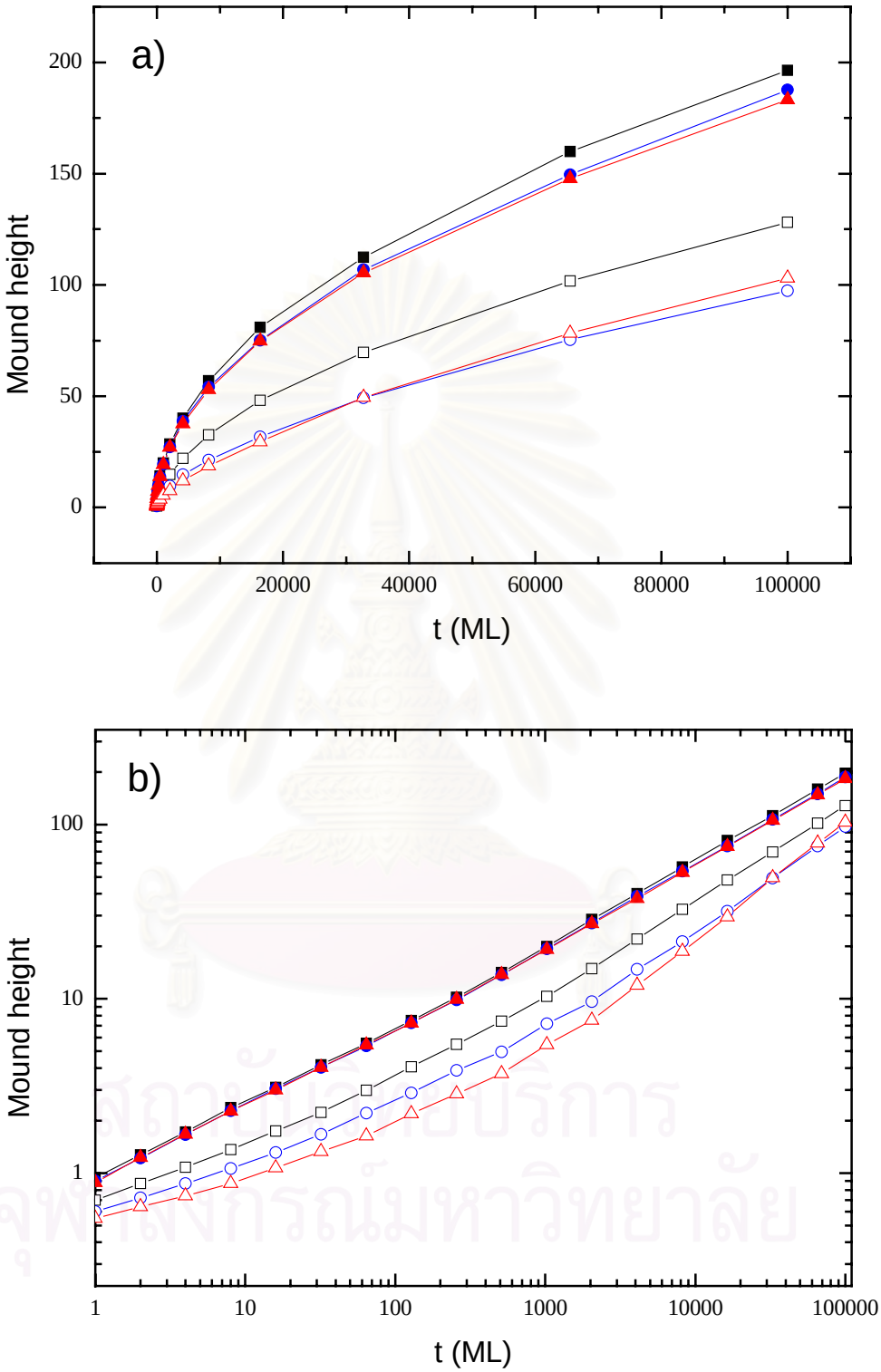

Figure 4.9: The evolution of the average mound height of the system with P_s=0.1 (filled symbol) and 0.5 (open symbol) at T=600 (square), 650 (circle), and 700 K (triangle). a) normal scale b) log-log scale

increases continuously with higher rate at initial and then slows down at later time. Obviously, the mound height of a system with P_s=0.1 is greater than that of P_s=0.5 for each T. Since in a system with high barrier the number of diffusing atoms that successfully hop down to fill up the grooves is less than that with lower barrier, the mound height of a system with high barrier is certainly greater than that with lower barrier.

From our study of the time evolution of mound radius and mound height, we can divide the growth process into two stages. At first, there are mound formations and then the individual mound coarsens together resulting in the increase of mound radius in this stage. Afterwards, coarsening rate becomes extremely slow. The mound radius becomes approximately constant at this point. Since the mound height increases continuously while the mound radius is a constant value, in this second stage the individual mound only grows vertically as if each mound is a separated system.

4.3 Scaling

To gain a deeper understanding of MBE growth under the effects of the ES barrier, scaling properties are studied in this section. Plots of the interface width versus time for P_s=0.1 (strong barrier) and P_s=0.5 (moderate barrier) at T=600 and 650 K are shown in Fig. 4.10. From Eq. (2.6), the growth exponent can be obtained from slope of the plot of interface width as a function of time at $t \ll L^z$. However, there seems to be a crossover at $t \sim 1000$ MLs in the plot in Fig. 4.10. From the study of time evolution of mound radius and mound height in Fig. 4.8 b) and Fig. 4.9 b), it can be concluded that the coarsening process of mounds in a system under ES barrier drastically slows down around 1000-3000 MLs. It is, therefore, possible that the scaling behavior of the MBE model under the effects of the ES barrier changes when the mounds stop coalescing. To avoid this crossover, we chose the time range between 2000 and 10^5 MLs for the slope calculation. Values

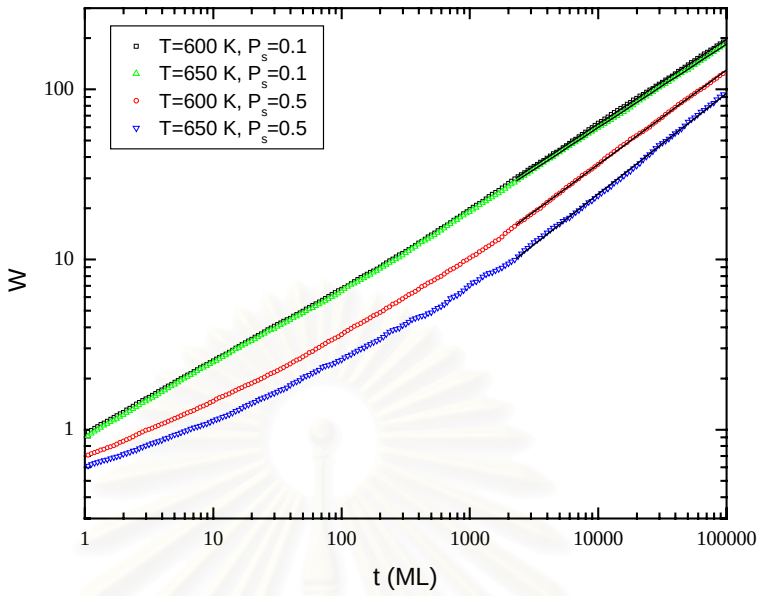

Figure 4.10: The interface width as a function of time of the systems with ES barriers.

of the growth exponent (β) extracted from these plots are all approximately 0.5 (0.56 for T=600 K and P_s=0.5, 0.50 for T=600 K and P_s=0.1, 0.59 for T=650 K and P_s=0.5, 0.49 for T=650 K and P_s=0.1). We have known that β=0.5 is a special characteristic of the RD model, where atoms are incorporated at random deposition sites without any diffusion. It is rather puzzling that the MBE growth with ES barrier model where atoms on the surface can hop continuously behaves similar to the RD model. In order to study this aspect in more details, other exponents (α and z) are calculated by performing data collapses. Figure 4.11 shows the data collapses for 7 sets of data at different time between 128 and 8192 MLs at T=600 (main panel) and 650 K (inset) for P_s=0.5. The same thing for P_s=0.1 is shown in Fig. 4.12. The roughness exponents α and the dynamical exponents z extracted from these plots are quite large (ranging from 3.2 to 3.6 for α and 6.4 to 7.1 for z) comparing with ones of systems without ES barriers. A collection of critical exponents, i.e. α, β, and z, extracted from Figs. 4.11 and 4.12 is shown in Table 4.1, where β is calculated from the ratio of α to z.

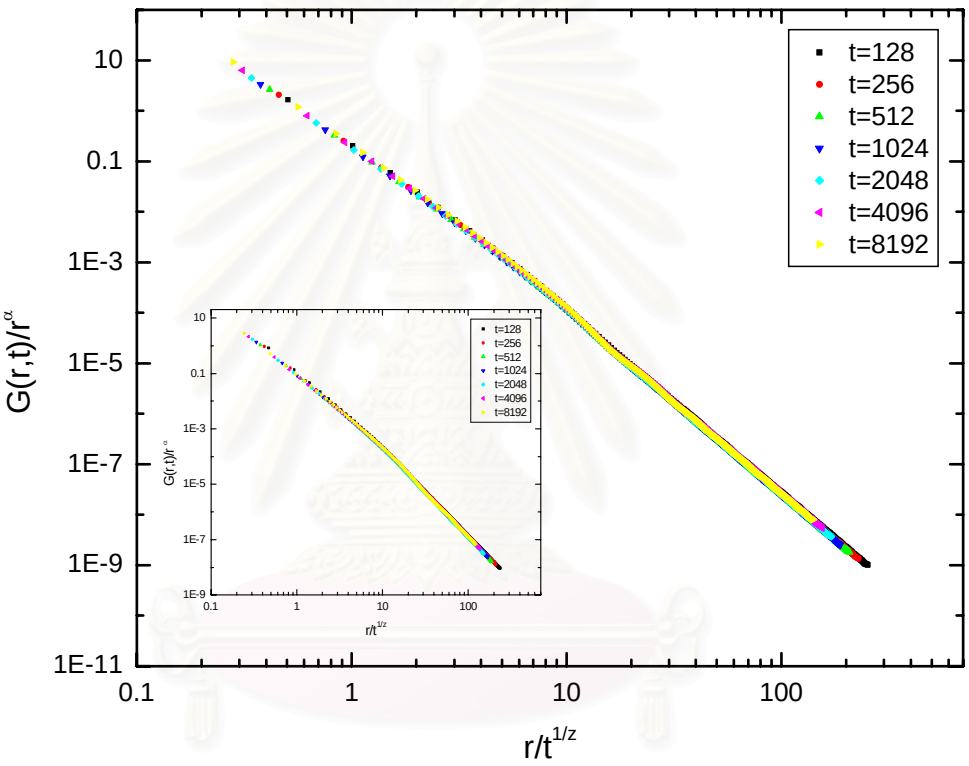

Figure 4.11: The data collapses of the systems with P_s=0.5 at T=600 (main panel) and 650 K (inset). Each collapse contains data for 7 times from 128 to 8192 MLs.

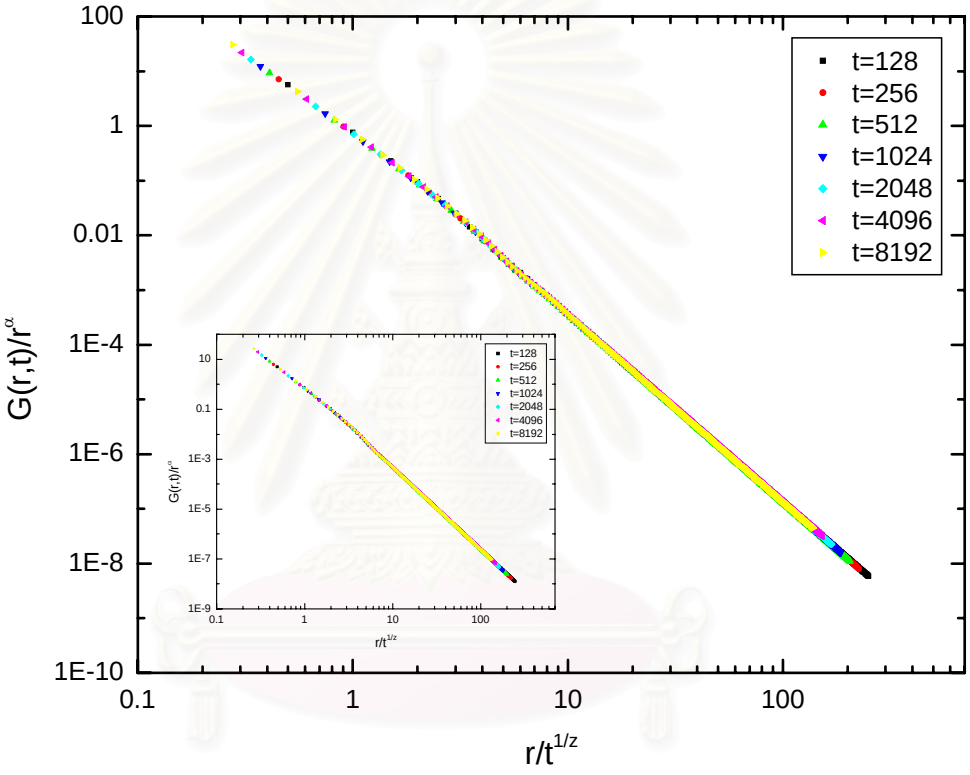

Figure 4.12: The data collapses of the systems with P_s=0.1 at T=600 (main panel) and 650 K (inset). Each collapse contains data for 7 times from 128 to 8192 MLs.

We note that from this table β is also very close to 0.5 whereas α and z are large but finite. Actually, in the RD model, β is equal to 0.5 while α and z are infinite. Interestingly, the growth exponents of both the MBE model with ES barriers and the RD model are approximately the same, whereas the roughness and the dynamical exponents are quite different. From the similarity of one critical exponent, we deduce that both models share some similarity, which we will discuss this at the end of this chapter.

To verify that α and z are indeed finite, we extend the simulation time to 10^5 MLs. The data collapses for 8 sets of data at different time between 1024 and 10^5 MLs at T=600 and 650 K for P_s=0.5 and P_s=0.1 were performed. The critical exponents extracted from these plots are shown in Table 4.2. We found that α and z increase from the value at the early time in Table 4.1; however, they still remain finite. Moreover, the growth exponents remain approximately 0.5 (0.55 for T=600 K and P_s=0.5, 0.49 for T=600 and P_s=0.1, 0.57 for T=650 K for T =650 K and P_s=0.5, 0.49 for T=650 and P_s=0.5). Obviously, due to the difference of α and z the MBE model with ES barriers is not exactly the same as the RD model.

Analyzing the correlation length and mound radius in Fig 4.13, we found that there are some similarities between the MBE model with ES barriers and the RD model. For the system without ES barriers (top line), the correlation length increases continuously through the simulation and finally it will extend to the size of a substrate. This means that the distance that atoms correlate to each other will extend to the entire system eventually. However, for the system with ES barriers, the correlation length increases at initial time and then seems to be saturated at some point. This shows that the correlation length cannot exceed a certain limit. Inaddition, we note that the correlation length of the system with ES barriers is always less than the mound radius of that system. It implies that in the growth process of system with ES barriers, individual mound grows independently and have no correlations with other mounds like the growing behavior of the RD model. This is the cause of β=1/2. However, from the non zero value and the

limiting to mound radius of the correlation length, there are correlations among lattice sites in each mound. It is the different behavior between the two models and is the reason why α and z in the MBE with ES model are not infinite like that of the RD model.

Exponents	T=600 K		T=650 K	
	P_s=0.1	P_s=0.5	P_s=0.1	P_s=0.5
α	3.43	3.62	3.3	3.2
β	0.49	0.51	0.49	0.50
z	7.0	7.1	6.8	6.4

Table 4.1: The critical exponents extracted from the data collapses in Fig. 4.11 and 4.12 for time range between 128 and 8192 MLs

Exponents	T=600 K		T=650 K	
	P_s=0.1	P_s=0.5	P_s=0.1	P_s=0.5
α	6.4	7.8	5.1	7.1
β	0.49	0.55	0.49	0.57
z	13.0	14.3	10.5	12.5

Table 4.2: The critical exponents extracted from the data collapses for time range between 128 and 10^5 MLs

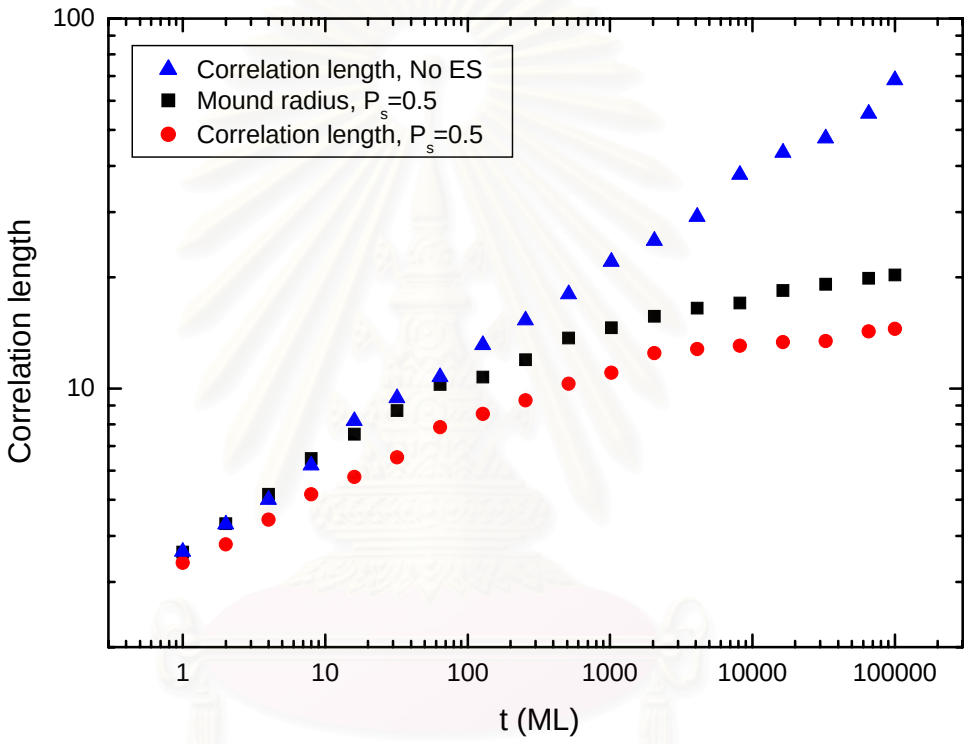

Figure 4.13: The correlation length as a function of time from systems with (circle) and without (triangle) ES barrier. The middle line (square) presents the evolution of mound radius.

Chapter 5

Conclusions

The aim of this thesis is to determine the effects of the Ehrlich-Schwoebel barrier on molecular beam epitaxy growth by using computer simulations. First, the MBE model, which attempts to include essential processes of the MBE growth such as deposition and diffusion, was studied. The MBE model was simulated under various conditions to study two main properties, i.e. the morphology and the scaling behavior. Moreover, the relation between the surface diffusion length, the displacement that a freshly deposited atom can diffuse before being incorporated into a growing film, and the substrate temperature, a controllable parameter in real experiments, was determined. To study the effects of ES barriers on MBE growth, the basic MBE model was modified. The ES barrier is included into the model through the tunneling probability. We found that there are mound formations in systems with ES barriers. The evolution of mound properties, i.e. the average mound radius and the average mound height, was then studied.

For systems without ES barriers, surface morphologies at various substrate temperatures were obtained. It is obvious that at low substrate temperature, i.e. 450 K, the surface is very rough and it becomes smoother when substrate temperature increases. We can divide these temperature-dependent morphologies to three main regimes. The first regime is at low temperature, at approximately 450 K. In this regime, surface diffusion is very rare so surfaces are very rough. The second regime is at intermediate temperature where surface diffusion has more effects in the growth process, so surfaces at this regime are smoother than ones

at low temperature regime. It should be noted, however, that these intermediate-temperature morphologies are still kinetically rough surfaces. The third regime is at high temperature where atoms have long surface diffusion length. Therefore, they can search for an energetically favorable position to stick, so the surfaces become extremely smooth as the growth process becomes a layer-by-layer growth.

Keeping track of each freshly deposited atom until it is incorporated and becomes a part of the film in simulations, we found that surface diffusion length ℓ_d increases with increasing substrate temperature T as $\ell_d \propto e^{-A/T}$ when A is a constant. Consequently, surface morphologies become smoother when T is higher, because atoms can search for the most energetically favorable positions.

For systems with ES barriers, obviously there are mound formations. Mound properties such as the average mound radius and the average mound height were studied by using the height-height correlation function $H(r)$. We found that systems with strong barriers have a narrower and higher mound structure than ones with weaker barriers because atoms can better overcome the weaker barriers to hop down to fill up the grooves. Consequently, the coarsening rate of systems with weaker barriers is faster than that with strong barriers.

From our study of the time evolution of mound radius and mound height, we can divide the growth process into two stages. At first, there are mound formations and then the individual mound coarsens together resulting in the increase of mound radius in this stage. Afterwards, a coarsening rate becomes extremely slow so the mound radius becomes approximately constant at this point. Since the mound height increases continuously while the mound radius is a constant value, in this second stage the individual mound only grows vertically as if each mound is a separated system. Since each mound grows independently like growth manner of the RD model, the growth exponents of the systems with ES barriers are very close to 0.5. It is important to note that the growth exponent of the RD model is equal to 0.5 while the roughness and the dynamical exponent are infinite. Strikingly, the roughness and the dynamical exponent of systems with ES barriers are indeed

finite, so growth manners of both the MBE model with ES barriers and the RD model are not exactly the same.

Calculating the correlation length of systems with ES barriers, we found that the correlation length is not equal to zero while it is exactly zero in the RD model. In summary, individual mound of systems with ES barriers grows independently like the growth behavior of the RD model. However, there are correlations among lattice sites in each mound. This makes the MBE model with ES barriers different from the RD model.

Since the model we use in this study requires so much time in simulations and there is also a problem with the limitation of computer resources, in this work we perform our simulations only in one dimensional substrate systems. In the future, substrates can be extended to two dimensions to compare simulated results with real experimental results. In addition, limit of height that a diffusing atom can hop should be considered in order to make the model more realistic.

References

[1] Das Sarma, S., Punyindu, P., and Toroczkai, Z. Non-universal mound formation in non-equilibrium surface growth. *Surf. Sci.* **457** (2000): L369-L375.

[2] Schinzer, S., Kinne, M., Biehl, M., and Kinzel, W. The role of step edge diffusion in epitaxial crystal growth. *Surf. Sci.* **439** (1999): 191-198.

[3] Ramana, M. V., and Cooper, B. H. Instability in molecular beam epitaxy due to fast edge diffusion and corner diffusion barriers. *Phys. Rev. Lett.* **83** (1999): 352-355.

[4] Khor, K. E., and Das Sarma, S. Quantum dot self-assembly in growth of strained-layer thin films: A kinetic monte carlo study. *Phys. Rev. B* **62** (2000): 16675-16664.

[5] Long, F., Gill, S. P. A., and Cocks, A. C. F. Effect of surface-energy anisotropy on the kinetics if quantum dot formation. *Phys. Rev. B* **64** (2001): 121307-121310.

[6] Ehrlich, G., and Hudda, F. G. Atomic view of surface self-diffusion. Tungsten on Tungsten. *J. Chem. Phys.* **44** (1966): 1039-1043.

[7] Schwoebel, R. L., and Shipsey, E. J. Step motion on crystal surfaces. *J. Appl. Phys.* **37** (1966): 3682-3686.

[8] Das Sarma, S. Growth models for virtual molecular beam epitaxy. *Computational Materials Science* **6** (1996): 149-151.

[9] Das Sarma, S., Lanczycki, C. J., Kotlyar, R., and Ghaisas, S. V. Scale invariance and dynamical correlations in growth models of molecular beam epitaxy. *Phys. Rev. E* **53** (1995): 359-388.

[10] Lanczycki, C. J. *Nonequilibrium interface growth: Roughening, coarsening and scale invariance.* Doctoral dissertation, Faculty of the Graduate School, University of Maryland, 1995.

[11] Punyindu, P., Toroczkai, Z., and Das Sarma, S. Epitaxial mounding in limited mobility models of surface growth. *Phys. Rev. B* **64** (2001): 205407-205430.

[12] Stroscio, J. A., Pierce, D. T., Stiles, M. D., and Zangwill, A. Coarsening of unstable surface features during Fe(001) homoepitaxy. *Phys. Rev. Lett.* **75** (1995): 4246-4249.

[13] Barabási, A. -L., and Stanley, H. E. *Fractal Concepts in Surface Growth.* Cambridge: Cambridge University Press, 1995.

[14] Siegert, M., and Plischke, M. Solid-on-solid models of molecular-beam epitaxy. *Phys. Rev. E* **50** (1994): 917-931.

[15] Mottet, C., Ferrando, R., Hontinfinde, F., and Levi, A. C. Simulation of the submonolayer homo epitaxial clusters growth on Ag(110). *Eur. Phys. J. D* **9** (1999): 561-564.

[16] Schinzer, S., Kohler, S., and Reents, G. Ehrlich-Schwoebel barrier controlled slope selection in epitaxial growth. *Eur. Phys. J. B* **15** (2000): 161-168.

[17] Das Sarma, S., and Tamborenea, P. I. A new universality class for kinetic growth: One-dimentional molecular beam epitaxy. *Phys. Rev. Lett.* **66** (1991): 325-328.

[18] Tamborenea, P. I., and Das Sarma, S. Surface-diffusion-driven kinetic growth on one-dimentional substrates. *Phys. Rev. E* **48** (1993): 2475-2594.

[19] Wolf, D., and Villain, J. Growth with surface diffusion. *Europhys. Lett.* **13** (1990): 389-394.

[20] Das Sarma, S., and Punyindu, P. A discrete model for non-equilibrium growth under surface diffusion bias. *Surf. Sci.* **424** (1999): L339-L346.

[21] Das Sarma, S., Ghaisas, S. V., and Kim, J. M. Kinetic super-roughening and anomalous dynamic scaling in nonequilibrium growth models. *Phys. Rev. E* **49** (1994): 122-125.

[22] Vvedensky, D. D., Zangwill, A., Luse, C. N., and Wilhy, M. R. Stochastic equations of motion for epitaxial growth. *Phys. Rev. E* **48** (1993): 852-862.

[23] Piankoranee, S. *Persistance in thin film growth on pattern substrates.* Master's thesis, Faculty of Science, Chulalongkorn University, 2004.

Vitae

Soontorn Chanyawadee was born in March 6, 1980 in Nakhon Phanom. He received his bachelor degree of science (first class honor) in physics from Khonkaen University in 2001. He was supported financially by the Development and Promotion of Science and Technology Talents Project (DPST) during his study.